A STUDY OF BERYLLIUM AND BERYLLIUM-LITHIUM COMPLEXES IN SINGLE-CRYSTAL SILICON

by

Roger K. Crouch

Thesis submitted to the Graduate Faculty of the

Virginia Polytechnic Institute

in candidacy for the degree of

DOCTOR OF PHILOSOPHY

in

Physics

APPROVED: ______________________________

T. E. Gilmer, Jr., Chairman

______________________________ ______________________________

C. D. Williams J. R. Long

______________________________ ______________________________

D. S. Wollan J. A. Jacobs

TABLE OF CONTENTS

CHAPTER		PAGE
	TITLE	i
	TABLE OF CONTENTS	ii
	LIST OF FIGURES AND TABLES	iv
I.	INTRODUCTION	1
II.	SHALLOW IMPURITY STATES IN SILICON	5
	DONORS	5
	ACCEPTORS	7
III.	DESCRIPTION OF THE EXPERIMENT	13
	OPTICAL STUDIES	13
	ELECTRICAL MEASUREMENTS	16
	DOPING PROCEDURES	18
	ANNEALING AND QUENCHING PROCEDURES	18
IV.	RESULTS AND DISCUSSION	21
	BERYLLIUM	21
	BERYLLIUM-LITHIUM COMPLEXES	31
V.	PROPOSED MODELS	40
	BERYLLIUM	40
	Set I	40
	Set II	44

CHAPTER		PAGE
	BERYLLIUM-LITHIUM	46
	Set I	46
	Set II	49
VI.	SUMMARY	51
	REFERENCES	53
	ACKNOWLEDGEMENTS	57
	VITA	58

LIST OF FIGURES AND TABLES

FIGURE PAGE

1. The spin-orbit split valence band of silicon with associated acceptor states 8

2. Absorption spectra of Group III impurities and the beryllium associated impurities 11

3. Typical Hall shape with dimensions 17

4. Quenching arrangement 19

5. Parameter containing carrier concentration and temperature as a function of temperature for beryllium doped silicon 22

6. Hall mobility as a function of temperature for beryllium doped silicon 23

7. Typical beryllium spectrum showing Set I and Set II absorptions and the broad absorption band at 500 cm^{-1} 25

8. (a) Temperature dependence of absorptions due to Set I beryllium 27

(b) Temperature dependence of absorptions due to Set II beryllium 28

9. Effects of quenching and annealing on Set I and Set II beryllium 29

10. Effect of beryllium on oxygen in Czochralski-grown silicon 32

FIGURE PAGE

11. Parameter containing carrier concentration and temperature as a function of temperature for a beryllium-lithium sample 33
12. Hall mobility as a function of temperature for a beryllium-lithium sample 34
13. Typical spectrum showing Set I and Set II beryllium-lithium absorptions 36
14. Effects of quenching and annealing on Set I and Set II beryllium-lithium absorptions 37
15. Temperature dependence of Set I and Set II beryllium-lithium absorptions 38
16. Schematic model for neutral Set I beryllium 41
17. Schematic model for singly ionized Set I beryllium . . 43
18. Schematic model for neutral Set II beryllium 45
19. Schematic model for singly ionized Set II beryllium. . 47
20. Schematic model for neutral beryllium-lithium complex, Set I 48
21. Schematic model for neutral beryllium-lithium complex, Set II. 50

TABLE

1. General information about samples 14
2. Location and spacings of lines in beryllium and beryllium-lithium spectra 26

I. INTRODUCTION

Technological advancements in recent years have led to an ever increasing demand for new and better solid state electronic devices. To assist in the development of such devices, numerous studies on the electrical [1-4] and optical [5-6] properties of the basic semiconducting materials have been carried out. As the technology progressed in growing and purifying single-crystal silicon, it became possible to introduce various concentrations of specific impurities into the crystal and then to catalogue the properties of the silicon containing the known impurity. Initially, it was found that Group V impurities produced n-type silicon and Group III impurities produced p-type silicon. It was shown that effective mass theory [9-12] gave excellent agreement between predicted and measured values for the excited state spectra of shallow donors,* that is, Group V impurities. The rather large discrepancies between predicted and observed ground state energies were understandable due to the simplified potential assumed in effective mass theory. [12-13] When effective mass theory was applied to shallow acceptors, it gave relatively good qualitative predictions for the excited states; but it did not give good quantitative values. Acceptor states are quite complicated, and the theory is still undergoing development. [14-15]

---

*Shallow impurity states, either donor or acceptor, are those bound states whose binding energy is much less than band gap energy.

Other studies showed that oxygen was present in large quantities in Czochralski-grown silicon; but the oxygen was electrically inactive in most cases and only modified the infrared absorption spectra of silicon by introducing vibrational absorptions, primarily around 9 microns. [16-17] The oxygen almost certainly occupied an interstitial lattice site in one of the six equivalent sites around a Si-Si bond. [18]

When lithium is introduced as an impurity in silicon, it forms a complex with the oxygen which alters the electrical and optical properties. [19-21] The lithium occupies a tetrahedral, interstitial position and is described by effective mass theory. [21] In float-zone silicon, oxygen content less than 10^{16} cm^{-3}, the lithium gives rise to an energy level 0.032 eV below the conduction band. In Czochralski silicon, oxygen content typically 10^{18} cm^{-3}, the lithium energy level is located 0.039 eV below the conduction band. Further studies indicate that the 9 micron vibrational absorption of the interstitial oxygen is shifted to about 10 microns. [22] Lithium has also been used to compensate heavily doped p-type silicon in order to reduce free carrier absorption and to study pair formation between lithium and boron. Vibrational absorptions have been found which have an isotopic dependency on the lithium and the boron, and a tentative model has been presented for the Li-B complex. [23-25] Some recent work deals with vibrational absorptions due to carbon and carbon-oxygen impurities in silicon. [26]

Group II impurities such as zinc and beryllium have been studied in germanium [27-29] and have been found to produce acceptor levels which, to a first approximation, can be described by a helium model.* The Group II impurities, magnesium and beryllium, have been studied in silicon. [30-34] It is interesting to note that the magnesium produces n-type silicon and occupies an interstitial lattice site, while beryllium produces p-type silicon and is therefore believed to occupy a substitutional lattice site. Magnesium introduces two related donor states described by a helium model. Beryllium introduces two independent series of infrared absorptions, which are separated by about 40 meV, neither of which seem to have the associated, deeper level expected for the helium model. (While it is uncommon for an impurity to produce two independent levels, beryllium is not unique in this respect since sulfur introduces at least two independent donor levels.) [35] When lithium is introduced into a beryllium doped silicon sample, two new series of infrared absorptions are found at energies closer to the valence band edge, indicating lithium forms a complex with the beryllium.

---

*A helium model is essentially a system which can be treated as a doubly charged nucleus with two carriers (either holes or electrons depending on the nuclear charge) bound to it at low temperatures. The first electron (hole) will have excited state energies comparable to those predicted by the "hydrogen model;" the second electron (hole) will have a ground state energy about four times deeper than the first electron. Also, the energy spacings between the excited states of the second electron will be larger by a factor of four.

A study of the electrical and optical properties of beryllium and beryllium-lithium complexes in silicon was done to better understand the unusual properties associated with these impurities. The results of this study are presented and discussed in this thesis. Tentative models for the two beryllium and the two beryllium-lithium impurity sites are proposed.

II. SHALLOW IMPURITY STATES IN SILICON

DONORS

When Group V elements are placed into a substitutional silicon lattice site, four of the electrons in the outer shell of the impurity atom are needed to complete the covalent bonds with the four adjacent silicon atoms. The fifth electron, however, is bound by a coulombic attraction to the remaining charge on the impurity ion. If this system is treated as a hydrogenic atom, where the potential energy of the electron is modified by the dielectric constant of the material and effective mass replaces the free-electron mass, then the excited state spectrum associated with the impurity should be observed in the far infrared. Experimental data on the Group V impurities, phosphorous, antimony, and arsenic, convincingly demonstrate the existence of bound states as demanded by the hydrogenic model for donors.

The Schrödinger equation for the donor state wave functions has the form

$$\left(- \frac{\hbar^2}{2m} \nabla^2 + V(\vec{r}) + U(\vec{r}) \right) \psi(\vec{r}) = E\psi(\vec{r}) \tag{1}$$

where $V(\vec{r})$ is the periodic potential of an electron in a perfect silicon lattice and $U(\vec{r})$ is the additional potential due to the impurity ion. For large r

$$U(\vec{r}) = - \frac{e^2}{\kappa r} \tag{2}$$

where $\kappa \approx 12$ is the dielectric constant of silicon. In silicon, the energy band structure of the conduction band has been found to have six equivalent minima located along the < 100 > directions in k space.[12] It has been shown by Kohn and Luttinger[9] that the impurity wave functions have the approximate form

$$\psi_i(\vec{r}) = \sum_{j=1}^{6} \alpha_j F_j(\vec{r})\varphi_j(\vec{r}) \qquad i = 1,\ldots,6 \tag{3}$$

where $\varphi_j(\vec{r})$ is the Bloch wave function at the jth conduction band minimum and α_j are the numerical coefficients which describe the relative contributions of each of the six equivalent minima. The $F_j(r)$ is a "hydrogen-like" envelope function which, for a band minimum in the < 001 > direction, satisfies the following "effective mass" wave equation:

$$\left[-\frac{\hbar^2}{2m_t}\left(\frac{\partial^2}{\partial x_j^2} + \frac{\partial^2}{\partial y_j^2}\right) - \frac{\hbar^2}{2m_l}\frac{\partial^2}{\partial z_j^2} - \frac{e^2}{\kappa r}\right]F_j(\vec{r}) = EF_j(\vec{r}) \tag{4}$$

m_t and m_l are the transverse and longitudinal effective masses, respectively, having the approximate values $m_t = 0.19\ m_0$ and $m_l = 0.98\ m_0$,[37] where m_0 is the rest mass of the electron.

When various Group V impurities are observed experimentally, the excited state structure observed in the spectra are in excellent agreement with theoretical predictions resulting from approximate solutions of equations (4). Since the orbits of these excited states are quite large, the potential in equation (2) should describe the situation very well. However, the value of the ground

state energy is different for different impurities; but this is not unexpected, since for small values of r the assumption of a screened ion potential is very poor. Local strains, a varying dielectric constant, and numerous other complications arise in the immediate vicinity of the impurity ion. There are no adequate theories to predict the ground state energies of the various impurities.

ACCEPTORS

When Group III impurities are placed on substitutional lattice sites in silicon, the unsatisfied covalent bond associated with one of the adjacent silicon atoms is an available electron state which can accept an electron from the valence band. When an electron is taken from the valence band, the resulting positively-charged hole will have a coulombic attraction for the negatively charged impurity ion. Thus, an effective mass hydrogenic model can also be used to describe the acceptor states. While these states are analogous to the donor states in a general way, the theory must incorporate the complexity of the valence band near its maximum at $\vec{k} = 0$ (see fig. 1).

If spin is not included, the band is threefold degenerate at $\vec{k} = 0$; but when spin is included, the resulting sixfold degeneracy is split by the spin-orbit interaction into a fourfold degenerate $p_{3/2}$ band and a twofold degenerate $p_{1/2}$ band. The $p_{3/2}$ band corresponds to the atomic $J = 3/2$ states, and the $p_{1/2}$ band corresponds to atomic $J = 1/2$ states.

Because of the nature of this degeneracy (i.e., the fact that three different bands are involved), the effective mass theory is more

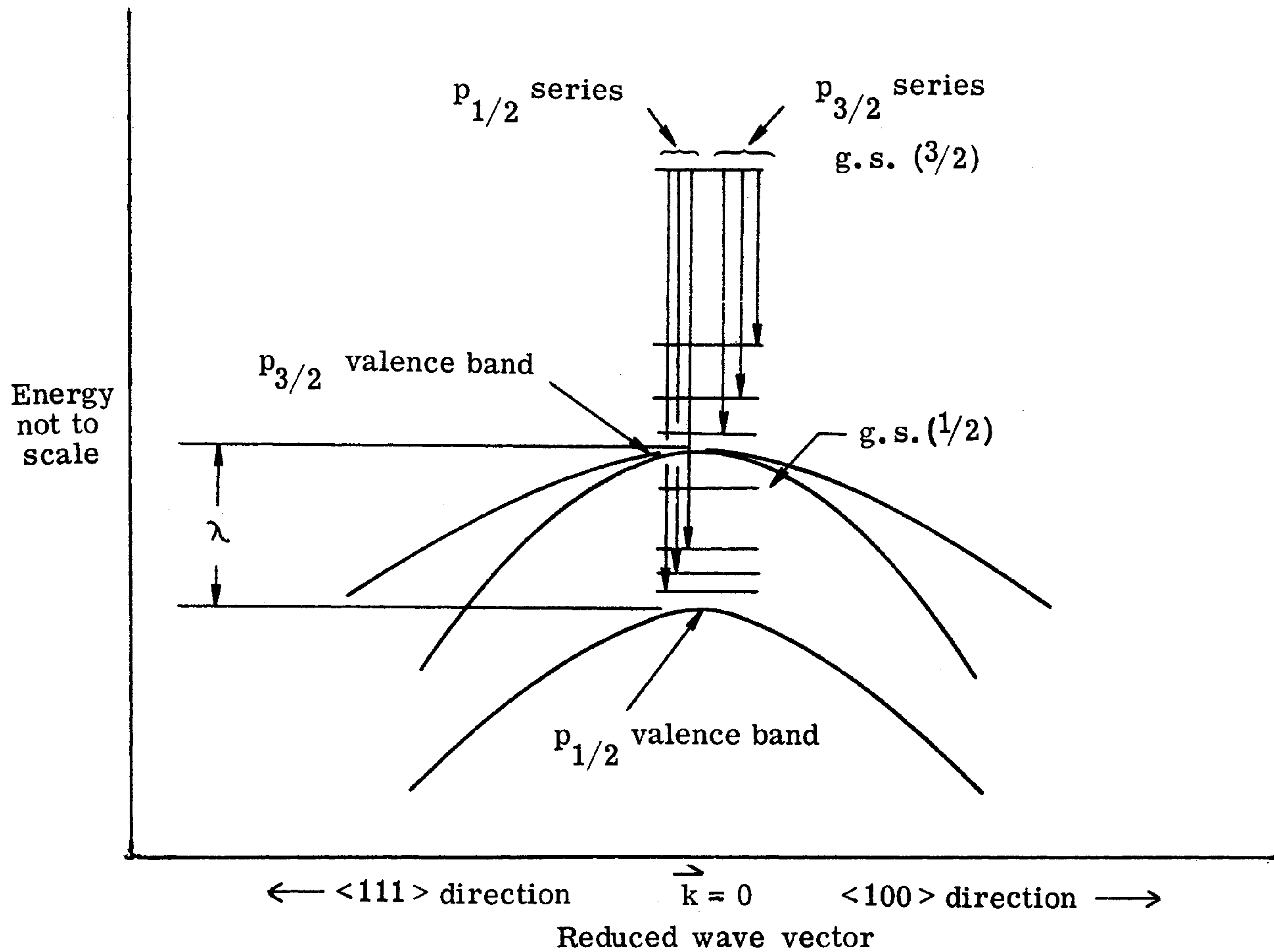

Figure 1.- The spin-orbit split valence band of silicon with associated acceptor states. Here g.s. is the ground state; λ is the spin-orbit splitting at $\vec{k}=0$; $\lambda \approx 44$ meV.

complicated for acceptors than for donors in silicon. Kohn [12] has treated the problem for silicon and found that the total wave functions of the acceptor states have structures given approximately by:

$$\psi_k(\vec{r}) = \sum_{j=1}^{6} F_j^k(\vec{r})\varphi_j(\vec{r}) \tag{5}$$

where the $F_j^k(\vec{r})$ are "hydrogenic" envelope functions modifying the Bloch functions, $\varphi_j(\vec{r})$. The index k distinguishes the degenerate functions among the impurity states, and the functions $F_j(r)$ are determined by the following six coupled "hydrogenic" effective mass wave functions:

$$\sum_{j'=1}^{6} D_{jj'}^{\alpha\beta}\left(\frac{1}{i}\frac{\partial}{\partial x^\alpha}\right)\left(\frac{1}{i}\frac{\partial}{\partial x^\beta}\right)F_{j'}(\vec{r}) + \frac{e^2}{\kappa r}F_j(\vec{r}) = (E + \lambda\epsilon_j)F_j(\vec{r}) \qquad \begin{matrix} j = 1,2,\ldots,6 \\ \alpha,\beta = 1,2,3 \end{matrix} \tag{6}$$

$D_{jj'}^{\alpha\beta}$ are numerical constants characteristic of the material and have dimensions of $\hbar^2/m$; $\epsilon_j = 0$ for $j = 1 - 4$ and $\epsilon_j = 1$ for $j = 5 - 6$; λ is the spin-orbit splitting at $\vec{k} = 0$ and κ is the dielectric constant. It may be shown that if λ were very large compared to E, the six equations would separate into four equations associated solely with the $p_{3/2}$ states and two equations associated solely with the $p_{1/2}$ states. In germanium, the spin-orbit splitting is about 30 times larger than the ionization energy and only four

equations are required to describe the acceptor states. For silicon, the energy of the acceptor states is on the order of 40-200 meV while λ is on the order of 40 meV; therefore, all six valence bands will enter with appreciable amplitude in the acceptor states in silicon.

When the experimental infrared absorption data are compared to the theoretical predictions, the agreement is qualitatively good; but there are small differences in the spacings of the excited state spectra for different impurities (fig. 2(a)). Also, as in the case of donors, the theory breaks down for small values of r; therefore, the depth of the ground state is chemically dependent. The acceptor-state equations for silicon, as is also the case for germanium, have been solved only approximately by variational techniques. However, it turns out that the theory and experiment do not agree as well for acceptor states in silicon as for these states in germanium, presumably due to the complexity introduced by the small value of the spin-orbit splitting in silicon.

As previously mentioned, the top of the $p_{3/2}$ valence band is fourfold degenerate. Many of the bound states associated with it are also fourfold degenerate. When external stresses are applied to silicon, the degeneracy of the localized states may be partially lifted. If the stress is applied uniaxially along the major axes of the crystals, it is theoretically possible to determine the degeneracies of the ground states and the excited states. Onton, et al.[8] have studied the Group III impurities (boron, aluminum, gallium and indium) in silicon by using these techniques. They have shown that all of these impurities are located in a

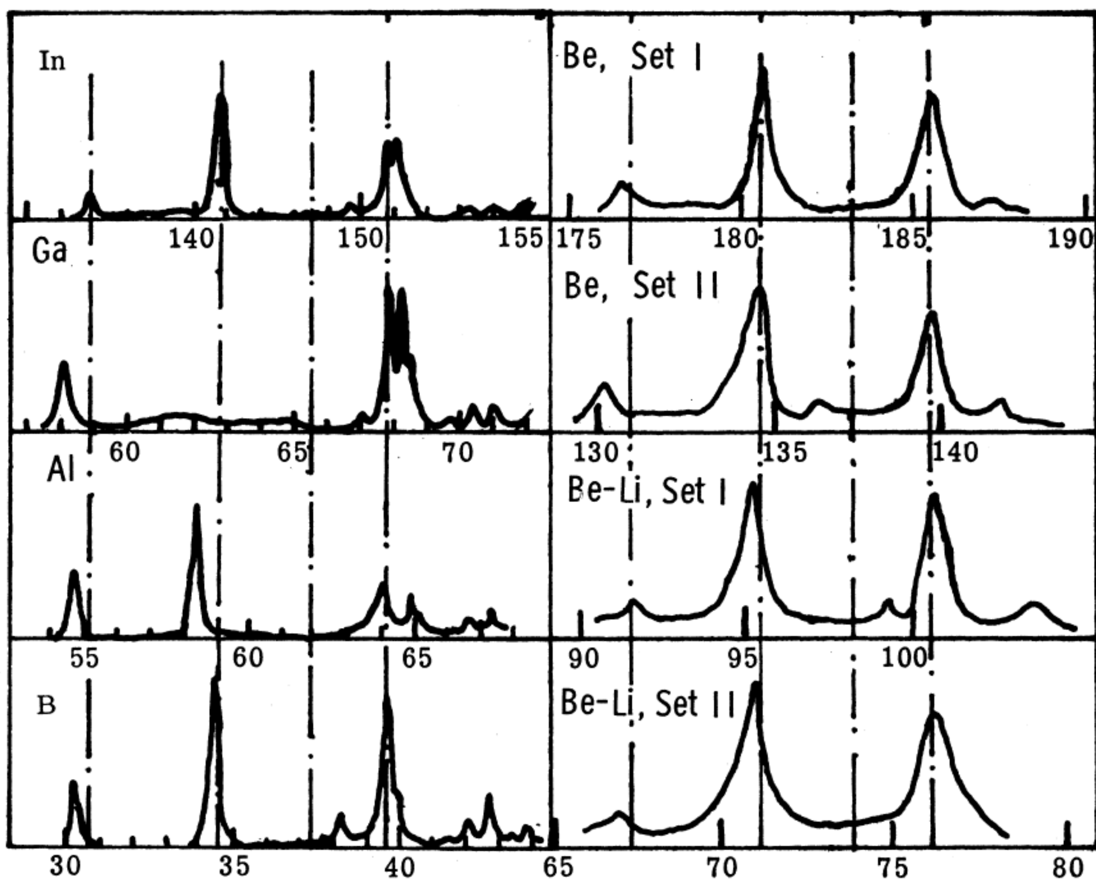

Figure 2a.- Lines associated with shallow acceptors (ref. 8).

Figure 2b.- Lines associated with beryllium complexes.

Vertical lines indicate the predicted location of lines using effective mass theory. All abscissa values are energy in meV, all ordinate values are schematic representations of relative absorption intensities.

Figure 2.- Absorption spectra of Group III impurities and the beryllium associated impurities.

tetrahedral lattice position. The ground state associated with this position is fourfold degenerate; and when stresses of sufficient magnitude are applied, the level is split into two twofold degenerate levels.

This section has presented a brief review of the theory for shallow impurity states in silicon. The ionization energies associated with the impurities reported in this thesis are large enough compared to the band gap energy to cause doubt as to the applicability of shallow acceptor theory; however, the excited state spectra of all the impurities studied appear to be in excellent agreement with the Group III impurities (see fig. 2). Because of this, at least the beryllium-associated impurity excited states have been regarded as shallow impurity states.

III. DESCRIPTION OF THE EXPERIMENT

OPTICAL STUDIES

Both Czochralski and float-zone single-crystal silicon [37] were used in preparing the test samples. Table 1 lists each sample reported, along with its method of growth, predominant impurity, resistivity prior to and after doping, doping time and temperature. The samples were polished disks 25.4 millimeters in diameter, and the thickness varied from about 0.5 millimeters up to 3.0 millimeters. Infrared absorption spectra were obtained over a range from 1.0 to 50 microns using two grating spectrophotometers. A Cary model 14 was used for the 1.0 - 2.5 micron range, and a Perkin-Elmer model 621 was used for the 2.5 - 50 micron range. Both instruments were purged by dry air during all runs. [38]

The infrared spectroscopy was performed at temperatures less than about 20° K for all figures presented in the thesis unless noted on the figure. The low temperature of the samples was attained through the use of a liquid helium dewar in which a copper sample holder was in contact with the cryogenic liquid. The temperature of the samples was not controlled in most cases and varied from around 8° K to 20° K depending upon the impurity concentration, thickness of the sample, and grade of thermal contact. Sample temperatures were measured with a commercially available germanium resistance thermometer. A piece of germanium is sealed inside a small copper block with a helium transfer gas inside. Four wires are mounted on the germanium to measure the

TABLE 1.- GENERAL INFORMATION ABOUT SAMPLES

(Information in colums 3-5 was supplied by manufacturer)

Sample identification	Data presented in figure number	Growth technique	Major impurity prior to doping	Resistivity prior to Be doping	Be doping		Resistivity after Be doping
					time, hr	temp., °C	
269-4	5,6	Float-zone	B	100 Ω - cm	1	1300	0.3 Ω - cm
X-9	7,8(b),9	Float-zone	P	100 Ω - cm	1	1300	0.25 Ω - cm
858-13	8(a)	Float-zone	P	800 Ω - cm	1	1300	Could not be measured
Ox-11	10	Czochralski	P	140 Ω - cm	2	1320	Could not be measured
X-10	11,12	Float-zone	P	100 Ω - cm	1	1300	0.2 Ω --cm
Ox-4	13	Czochralski	P	140 Ω - cm	2	1340	0.4 Ω - cm
422-14	14	Float-zone	P	260 Ω - cm	1 1/4	1340	0.2 Ω - cm
957-23	15	Float-zone	P	380 Ω - cm	1	1300	0.5 Ω - cm

resistance which has been previously calibrated as a function of temperature. The copper block is mounted against the silicon by using vacuum grease.

All plots of optical data are presented in terms of percent transmission rather than absorption coefficient as a function of wave number. Since the absorptions are very strong in most cases, errors in percent transmission (up to 5 units) would lead to large errors in absorption coefficient.[5] It can be shown that the absorption coefficient, α, is related to the light intensity by:

$$I = I_o \frac{(1 - R)^2 \exp(-\alpha t)}{1 - R^2 \exp(-2\alpha t)} \qquad (7)$$

where I is the intensity of the beam after passing through the sample, I_o is the incident beam intensity, R is the reflectivity of the sample surface, and t is the sample thickness. The percent transmission, T, is the ratio of the intensities.

$$T = \frac{I}{I_o} = \frac{(1 - R)^2 \exp(-\alpha t)}{1 - R^2 \exp(-2\alpha t)} \qquad (8)$$

Solving equation (8) for α gives

$$\alpha = \ln\left[\frac{(1 - R)^2 + \sqrt{(1 - R)^4 + 4T^2R^2}}{2T}\right] t^{-1} \qquad (9)$$

It is readily seen from equation (9) that if $R \ll 1$, α varies as the logarithm of the reciprocal of the transmission. Therefore, as T approaches zero, it can become very important that measurements of T become more accurate; yet, the sensitivity of the experimental setup is such that more accurate values of percent transmission cannot be measured. Since this study deals primarily with energy locations and relative absorption strengths, values of absorption coefficients would not lead to any significant new conclusions and percent transmission measurements would be just as informative.

ELECTRICAL MEASUREMENTS

Hall samples were cut in the standard bridge shape shown in figure 3. Contacts to the samples were made by sputtering aluminum on the tabs and annealing at 600° C for 15 minutes to form an eutectic bond between the aluminum and silicon. The leads were soldered to the aluminum-coated tabs with indium solder and a tesla coil was arced to each tab to help break down any rectifying contacts that still remained. Resistivity and Hall voltage were measured in a manner essentially the same as that described in reference 19. The magnetic field used for the Hall measurements was 2,740 gauss.

The resistivity of the optical samples prior to polishing was measured by a four-point probe as explained by Valdes.[36] The resistivity of some optical samples was not measured due to difficulty in establishing good electrical contacts.

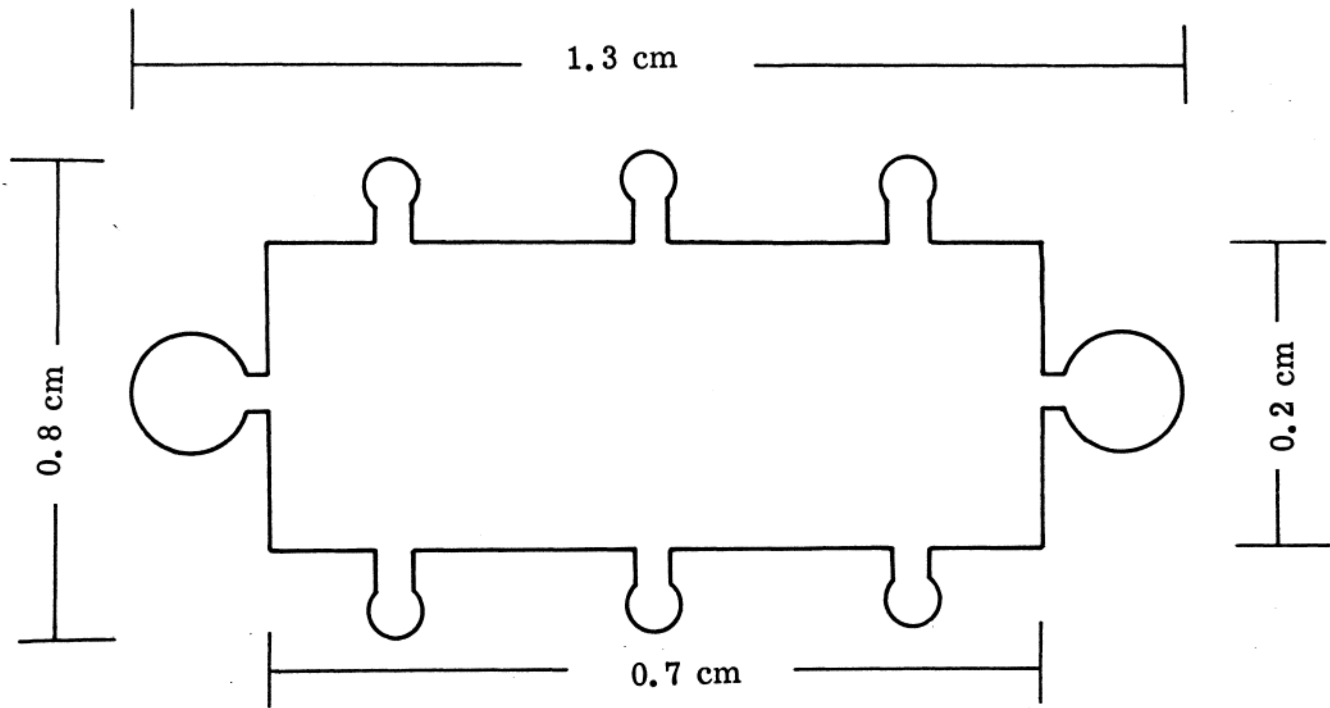

Figure 3.- Typical Hall shape with dimensions.

DOPING PROCEDURES

Beryllium.- Beryllium was thermally diffused into the silicon using the "sandwich" method.[30] A layer of beryllium was vapor deposited onto each silicon wafer. Two or more wafers were stacked with the plated sides adjacent and placed in a helium environment at temperatures of 1300° C to 1340° C for 1 to 2 hours (see table 1). The wafers were welded together during the dope and had to be sawed apart.

Lithium.- The most efficient way to introduce the lithium was to plate a "dummy" wafer on both sides with lithium and "sandwich" this dummy between two beryllium doped wafers. The "sandwich" was placed in a helium environment and heated at 600° C for 30 minutes. The two outer wafers were then turned over and heated for another 30 minutes. The lithium plated wafer was then removed, and the two doped wafers were annealed at 600° C for 30 minutes to assure a more uniform doping.

ANNEALING AND QUENCHING PROCEDURES

Samples to be annealed were placed between two high-purity wafers of silicon in a helium environment. This was done to reduce surface chemical reactions between stray impurities in the system and the doped sample.

For quenching, the samples were held against a cylindrical piece of graphite by means of a reduced pressure inside the graphite cylinder (see fig. 4). A thermocouple was placed against the silicon to allow temperature monitoring. This system was placed in a cylindrical quartz tube with a nitrogen gas stream flowing by the sample. The graphite was heated by means of an rf heater until the wafer reached the desired

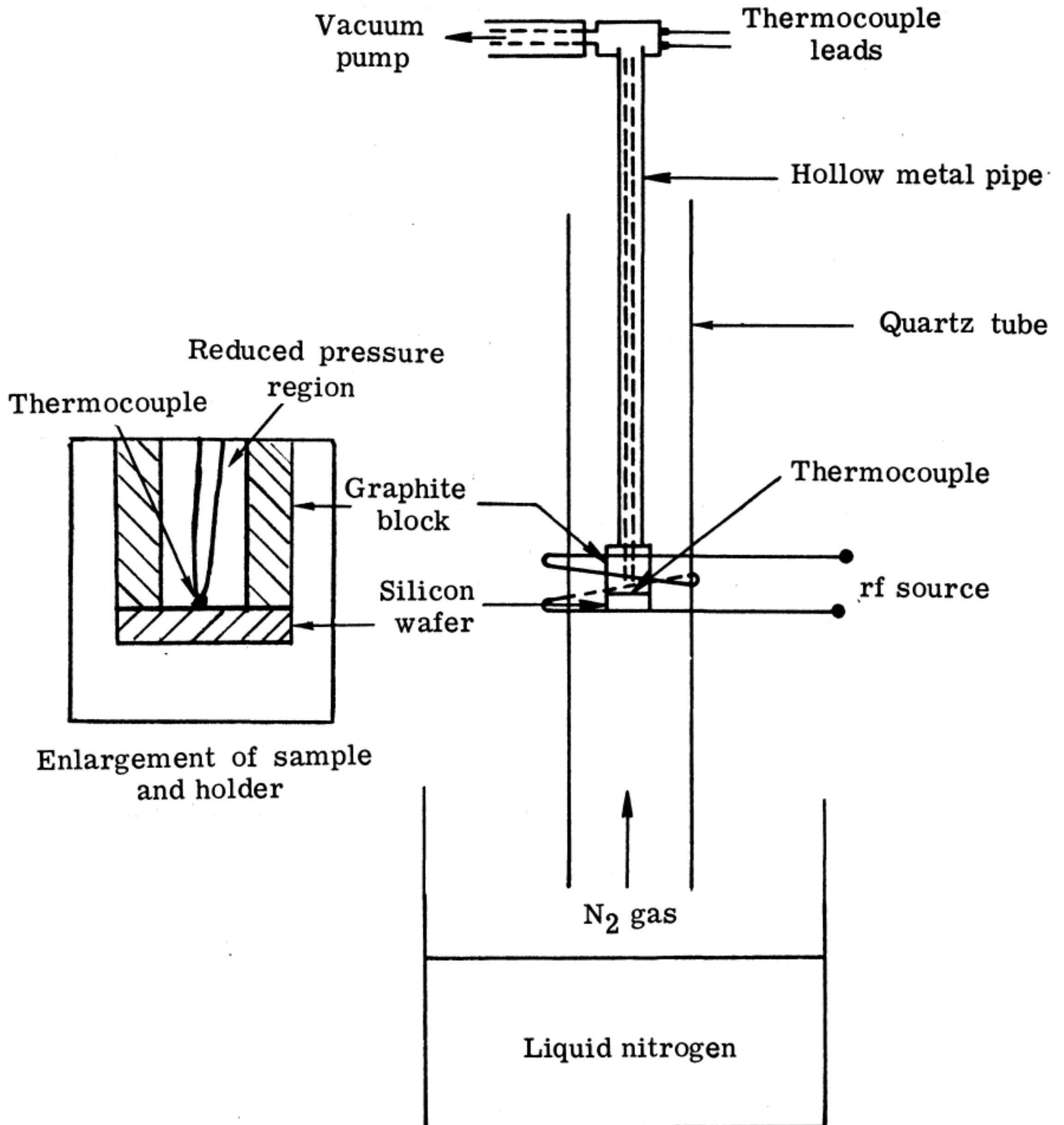

Figure 4.- Quenching arrangement.

temperature where it was held for about 3-5 minutes and dropped into a liquid nitrogen bath. In all cases the samples were brought back to room temperature before mounting in the cryostat.

IV. RESULTS AND DISCUSSION

BERYLLIUM

Beryllium can be introduced into silicon by thermal diffusion at a temperature of 1300° C to 1340° C. Typical calculations based on the Hall coefficient in the resultant p-type material is presented in figure 5. The ionization energy for the acceptor level, E_A, giving rise to these carriers is found to be on the order of 160 meV. Hall mobility,

$$\mu_H = \frac{R_H}{\rho} \qquad (10)$$

as a function of temperature typically looks like that shown in figure 6.

The temperature dependence of the mobility indicates the dominant free carrier scattering mechanism. If the scattering is primarily due to phonons, the mobility has a negative power dependency on the temperature; however, if ionized impurity scattering is dominant, the mobility will be a positive power function of the temperature.[39] Here it is noted that the mobility is primarily controlled by phonon scattering down to temperatures around 80° K. When silicon is heavily conpensated (on the order of 10^{16} cm^{-3}), the mobility is primarily controlled by phonon scattering down to temperatures of only 100° K or greater; therefore, the beryllium is typical of a p-type impurity with low or moderately low compensation levels.

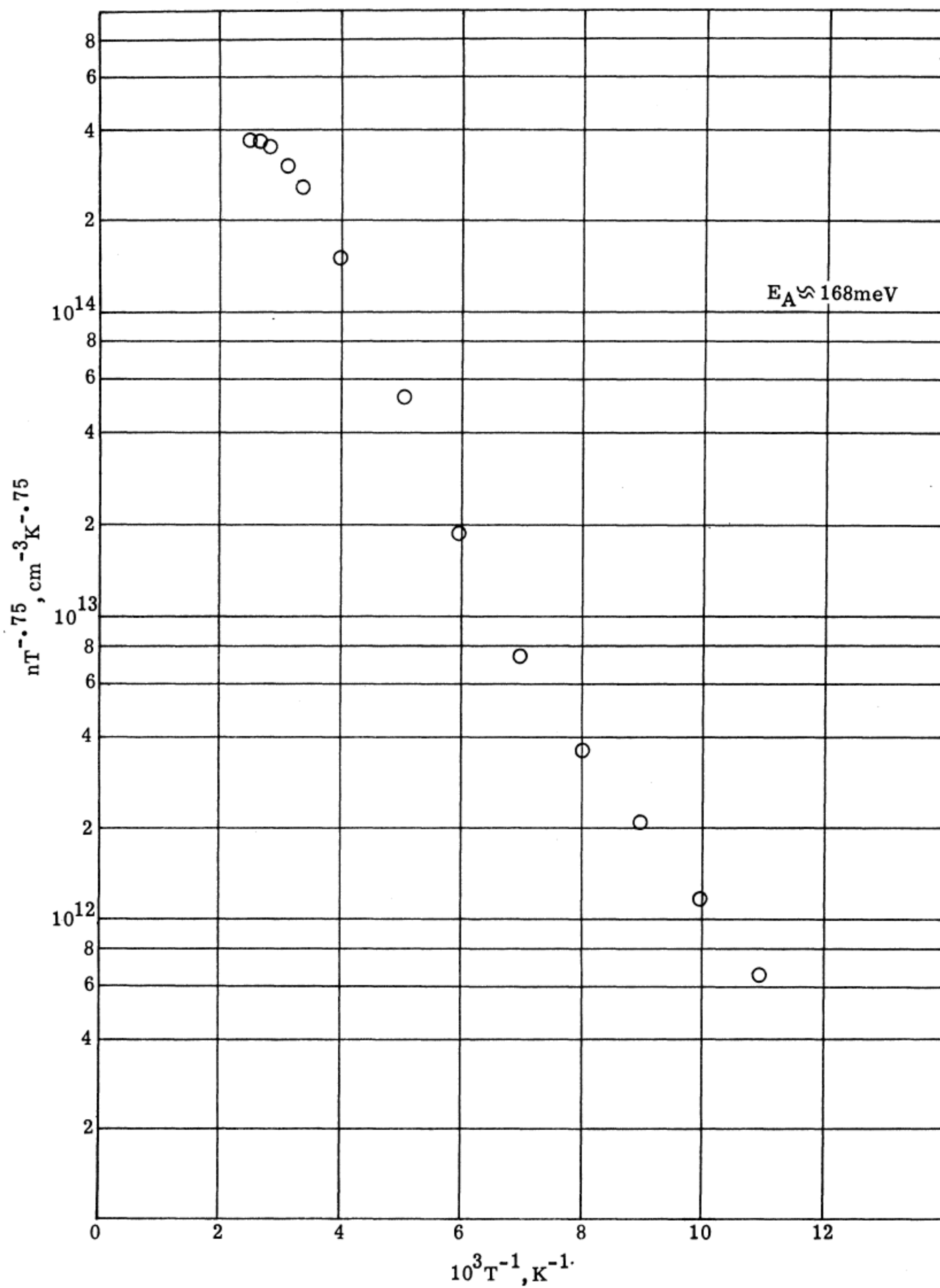

Figure 5.- Parameter containing carrier concentration and temperature as a function of temperature for beryllium doped silicon.

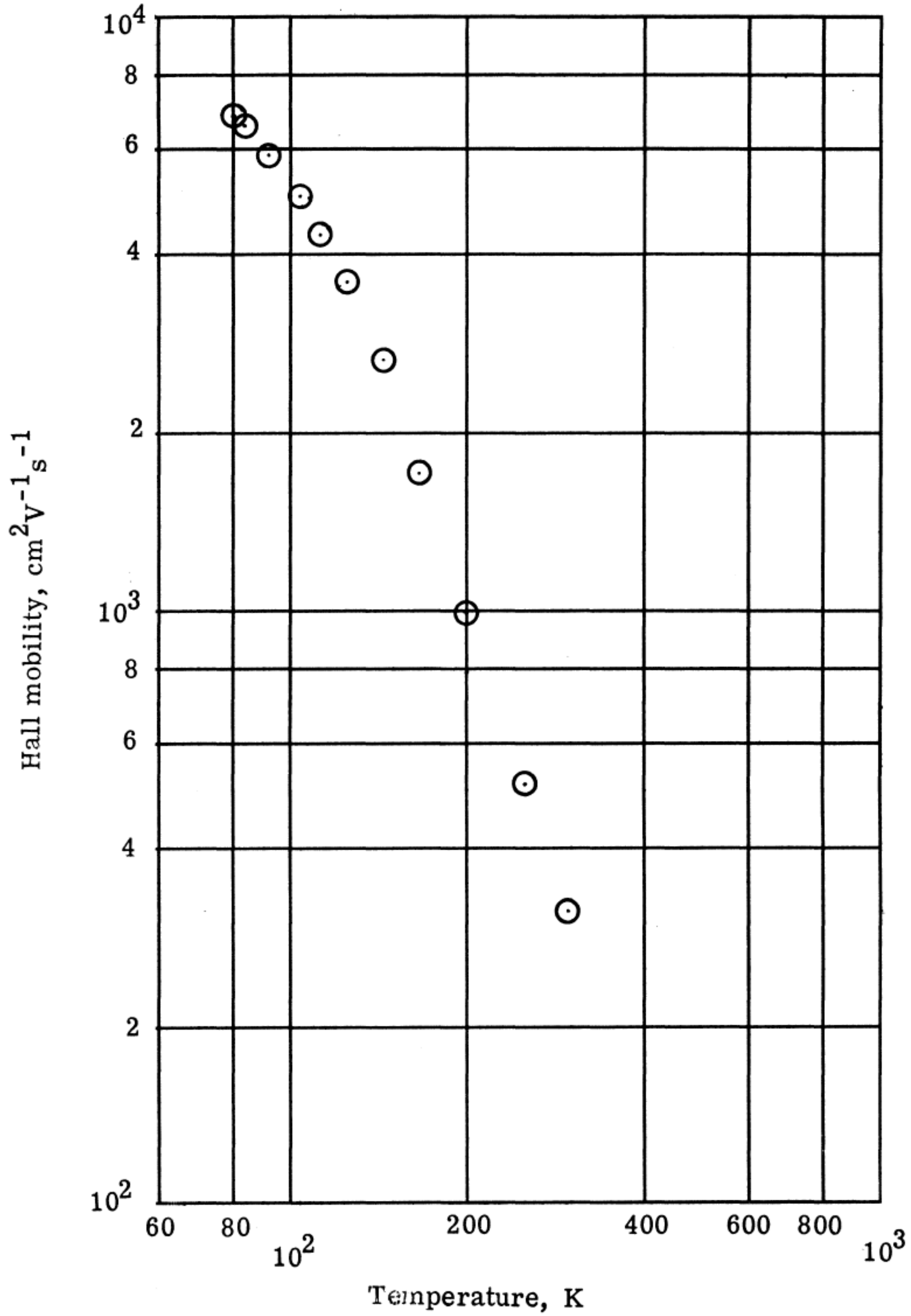

Figure 6.- Hall mobility as a function of temperature for beryllium doped silicon.

Absorption studies in the infrared region of beryllium in silicon at low temperatures show that there are two series of sharp absorptions, located around 1450 cm^{-1} and 1080 cm^{-1} (labeled Set I and Set II, respectively) and a single broad absorption centered on 500 cm^{-1} (see fig. 7). The spacings between absorptions are typical of the spacings observed for shallow acceptors in silicon as seen in table 2 and figure 2. If shallow acceptor theory is applied, these two series correspond to ionization energies of 191 and 145 meV, respectively. This is in acceptable agreement with the value obtained from the Hall measurements.

As the temperature of the sample is raised, the Set I and Set II lines broaden quite rapidly as shown in figures 8(a) and 8(b). Resolution of the lines above 100° K was not possible. However, the broad line at 500 cm^{-1} does not seem to change very much with temperature, indicating that it is probably a localized impurity vibrational absorption associated with one of the beryllium centers.[24-26]

As seen in table 2, the spacings of the major lines in the Set I and Set II absorptions are quite similar. The Set II series is always weaker than the Set I, never having an absorption intensity greater than about one-half that of Set I. When a beryllium doped sample is quenched from a temperature greater than about 600° C, the Set II series is drastically reduced or disappears while the Set I and 500 cm^{-1} lines increase slightly (fig. 9). When a sample is slowly cooled (on the order of 2 hours) from 600° C to room temperature, the Set II series absorption is increased to its maximum value relative

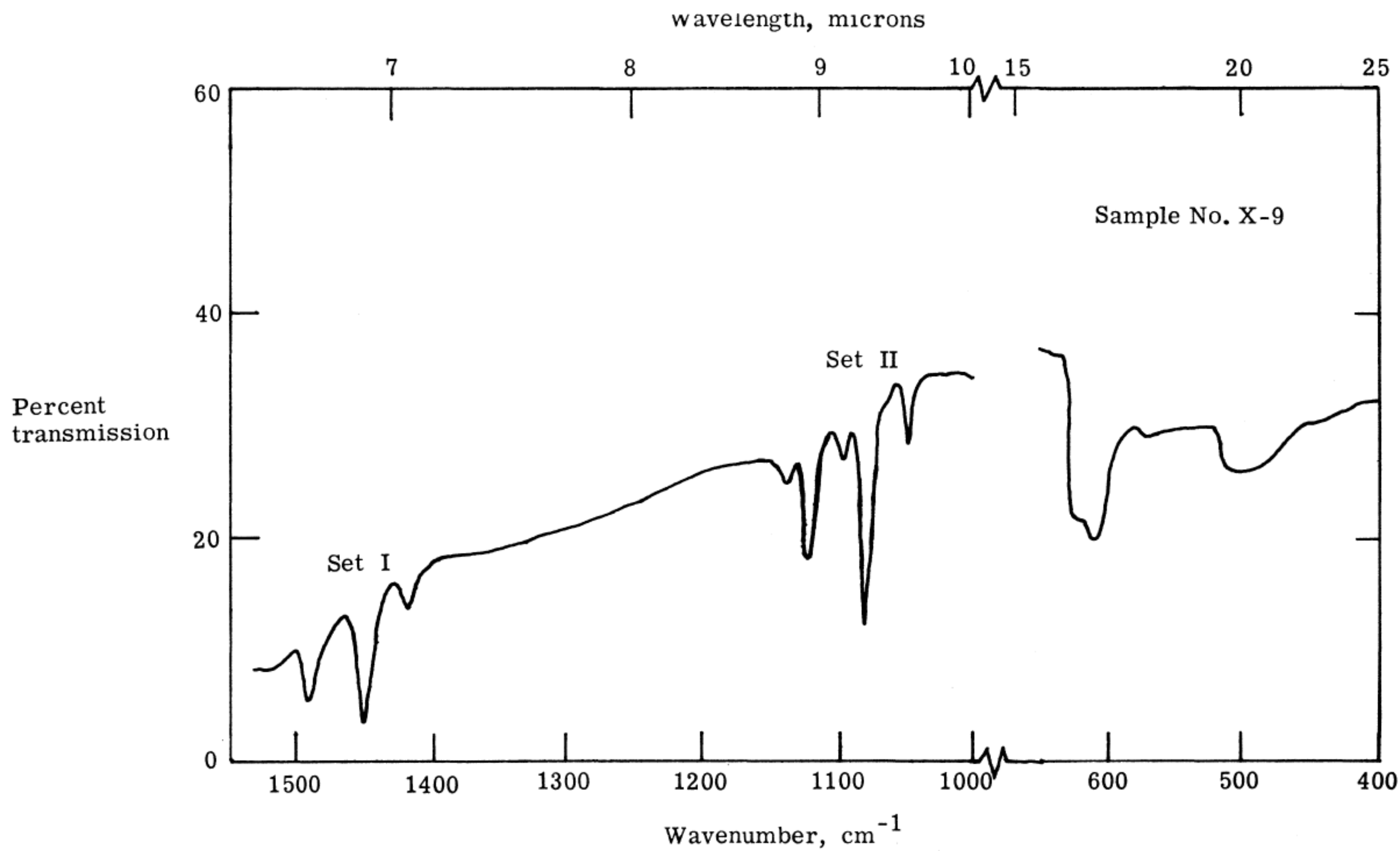

Figure 7.- Typical beryllium spectrum showing Set I and Set II absorptions and the broad absorption band at 500 cm^{-1}.

TABLE 2.- ENERGY LOCATION AND SPACINGS OF LINES IN TYPICAL BERYLLIUM AND BERYLLIUM-LITHIUM SPECTRA

(a) Energy location of lines for various impurities, meV.

Line number	Boron	Indium	Beryllium, Set I*	Beryllium, Set II*	Be + Li, Set I*	Be + Li, Set II*
1	30.38	141.99	176.6	130.2	91.8	67.0
2	34.53	145.79	180.3	134.4	95.1	70.8
3	38.35	149.74		136.4	99.1	
4	39.64 39.91	150.80 151.08	185.6	139.7	100.4	76.1
5	41.52	(152.8)				
6	42.50	153.27				
7	42.79			141.9	103.0	

*Line designations are arbitrary.

(b) Energy spacings between lines, meV.

Line number	Boron	Indium	Beryllium, Set I*	Beryllium, Set II*	Be + Li, Set I*	Be + Li, Set II*
Δ 12	4.15	3.80	3.7	4.2	3.3	3.8
Δ 23	3.82	3.95		2.0	4.0	
Δ 24	5.11	5.01	5.3	5.3	5.3	5.3
Δ 47	3.15			2.2	2.6	

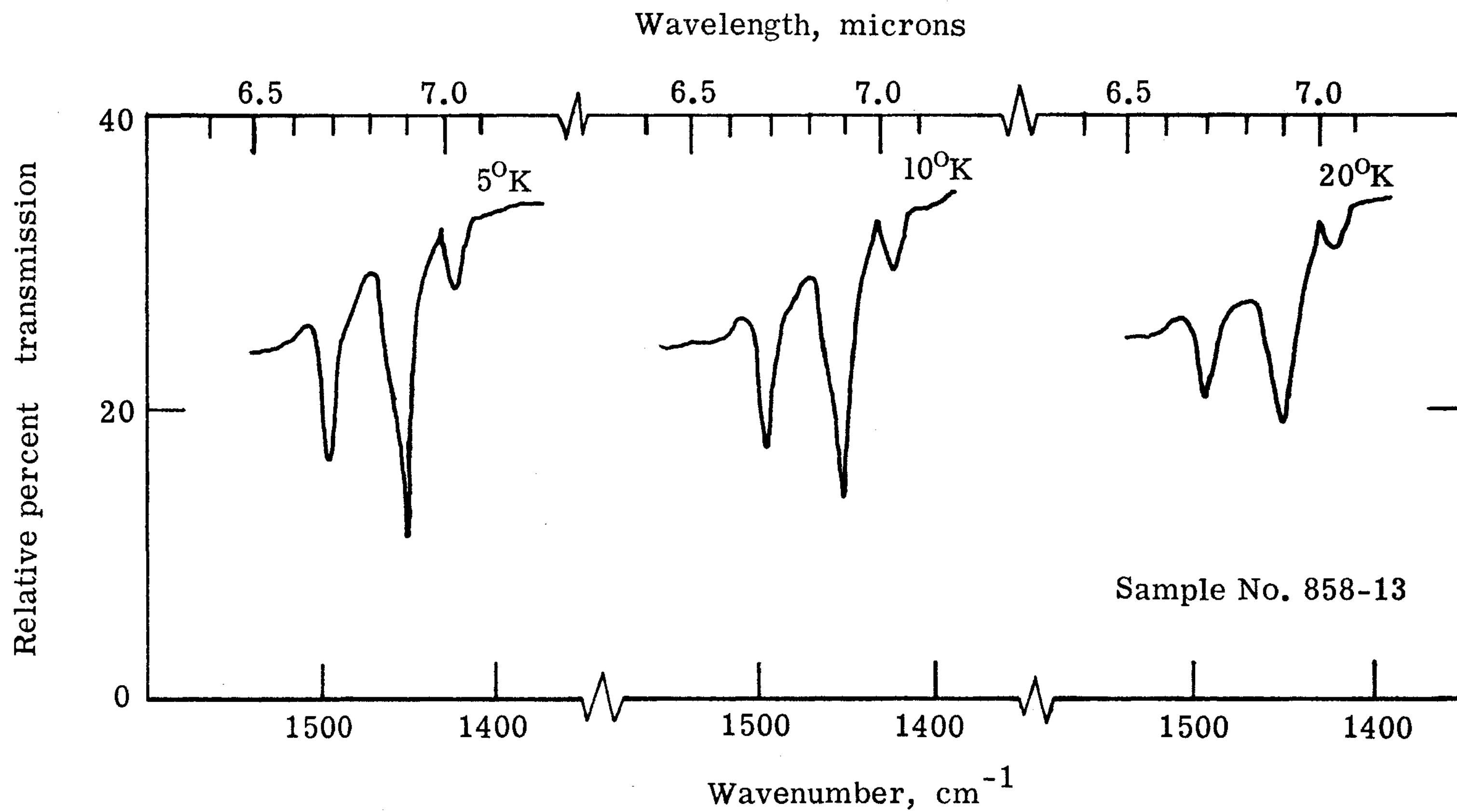

Figure 8(a).- Temperature dependence of absorptions due to Set I beryllium.

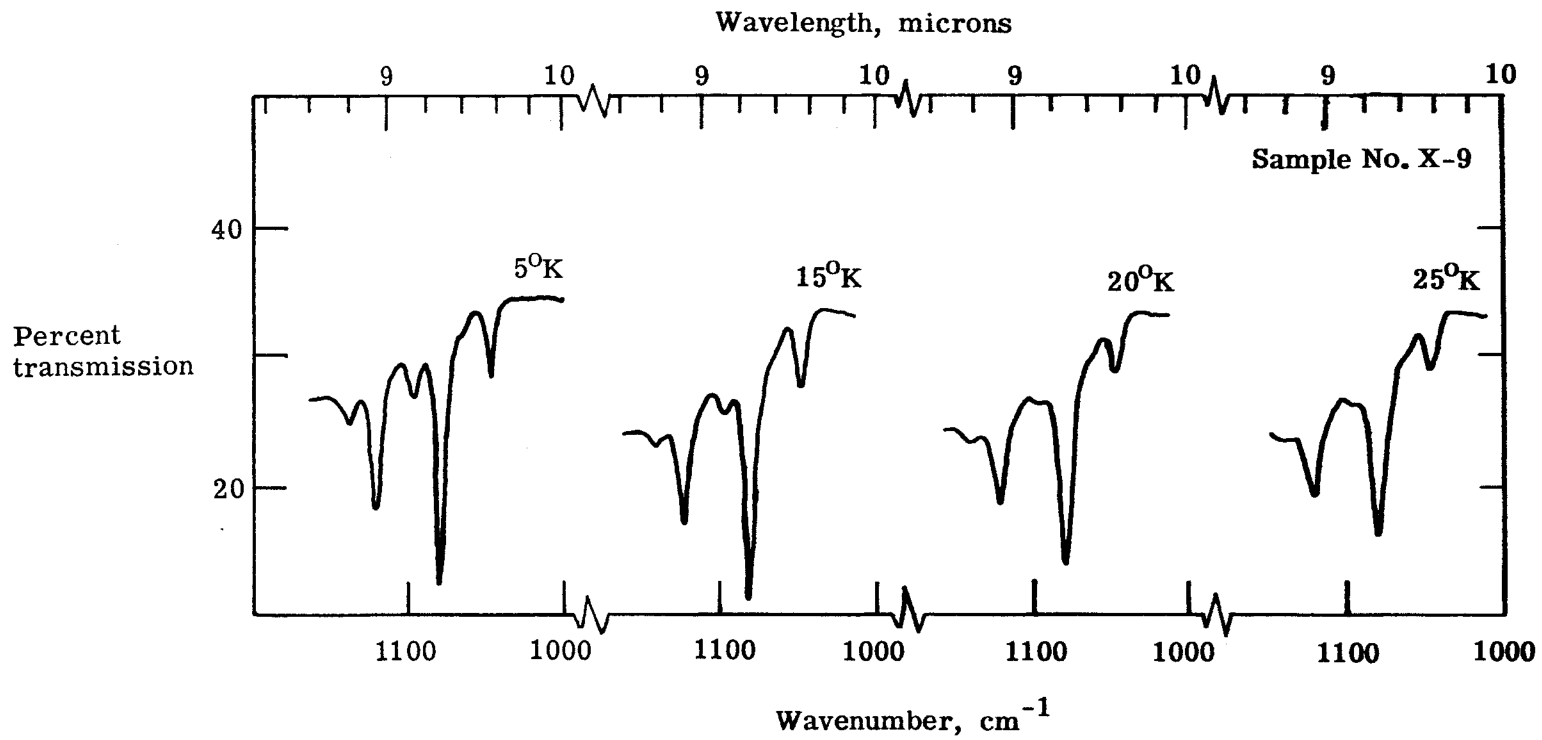

Figure 8(b).- Temperature dependence of absorptions due to Set II beryllium.

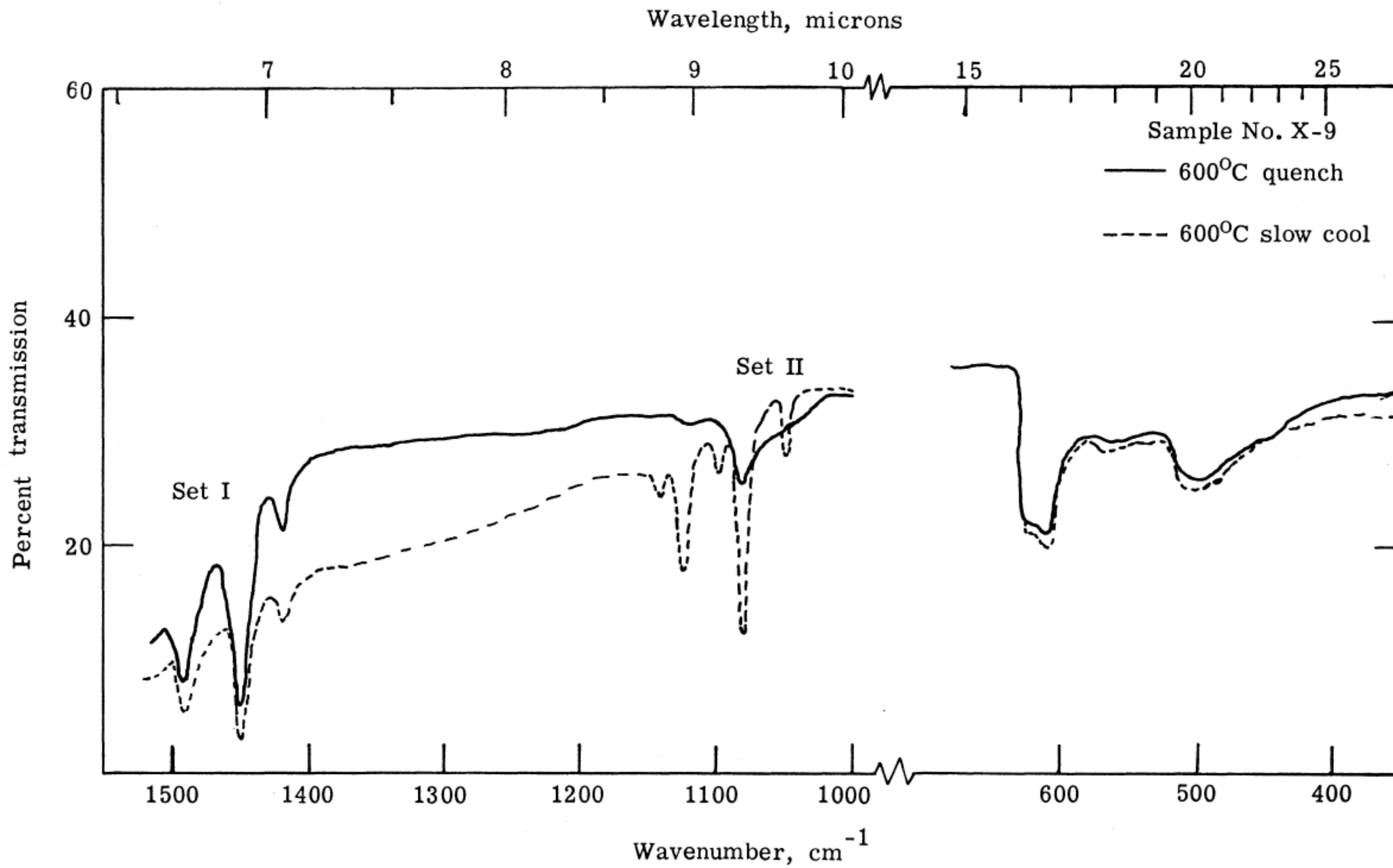

Figure 9.- Effects of quenching and annealing on Set I and Set II beryllium.

to Set I. Set I and the 500 cm^{-1} lines are slightly decreased in strength (fig. 9).

From these data it appears that the Set I and Set II series arise from two different configurations of the beryllium impurity atoms. Since the spacings between the lines are essentially the same and the ratio of the absorption coefficients can be changed, it is very unlikely that the Set II absorptions are the $p_{1/2}$ spectra as might be suspected at first. That is, transitions have previously been observed to states associated with the $p_{3/2}$ valence band and the $p_{1/2}$ valence band which are separated by about 44 meV (see fig. 1). However, it is unlikely that the spacings between lines would be so close, or that the relative strengths of absorption would be affected by heat treatment.

It might be noted that beryllium is not unique in introducing more than one independent impurity level spectrum. Sulfur, when introduced into silicon, gives rise to four donor levels, at least two of which are unrelated (i.e., not the second level of a "helium" model), and whose relative absorptions are dependent on temperature histories. [35]

Figure 9 indicates that the 500 cm^{-1} band is associated with the Set I impurity vibration since it generally tends to follow the behavior shown by Set I under quenching and annealing. When a beryllium doped sample is annealed (held at constant temperature for various times) at temperatures greater than 1000° C, the Set I and 500 cm^{-1} absorptions decrease at about the same rate, so that after about 4 to 6 hours they both completely disappear due to out diffusion of the beryllium.

When beryllium is introduced into Czochralski-grown silicon (oxygen content typically 10^{18} cm^{-3}), the 9 micron absorption associated with interstitial oxygen completely disappears (fig. 10). The beryllium spectra appears to be no different from that for the float-zone silicon (oxygen content less than 10^{16} cm^{-3}). Even after annealing for several hours to remove all the optically active beryllium, the 9 micron oxygen line is never fully recovered (i.e., the interstitial oxygen content in a position giving rise to the 9 micron line remains less than 0.1 its original value).

BERYLLIUM-LITHIUM COMPLEXES

When lithium is thermally diffused into silicon, it normally occupies an interstitial position and gives rise to a donor level. It is expected that lithium would compensate the beryllium impurities and allow study of the singly ionized beryllium states, expected if beryllium could be described by a helium model. After the lithium was introduced into beryllium doped silicon, the samples were still p-type after diffusion for 1 hour at 600° C. Calculations from Hall data (fig. 11) indicated that the holes were bound in a level with an ionization energy, E_A, of about 108 meV. This may be compared with ionization energies which would be expected from compensation of the helium model viz. energies around 800 meV. The mobility data shown in figure 12 exhibited very little of the ionized impurity scattering which would be expected for a highly compensated sample; in fact, the mobility in Be + Li samples was essentially the same as for comparably doped beryllium samples.

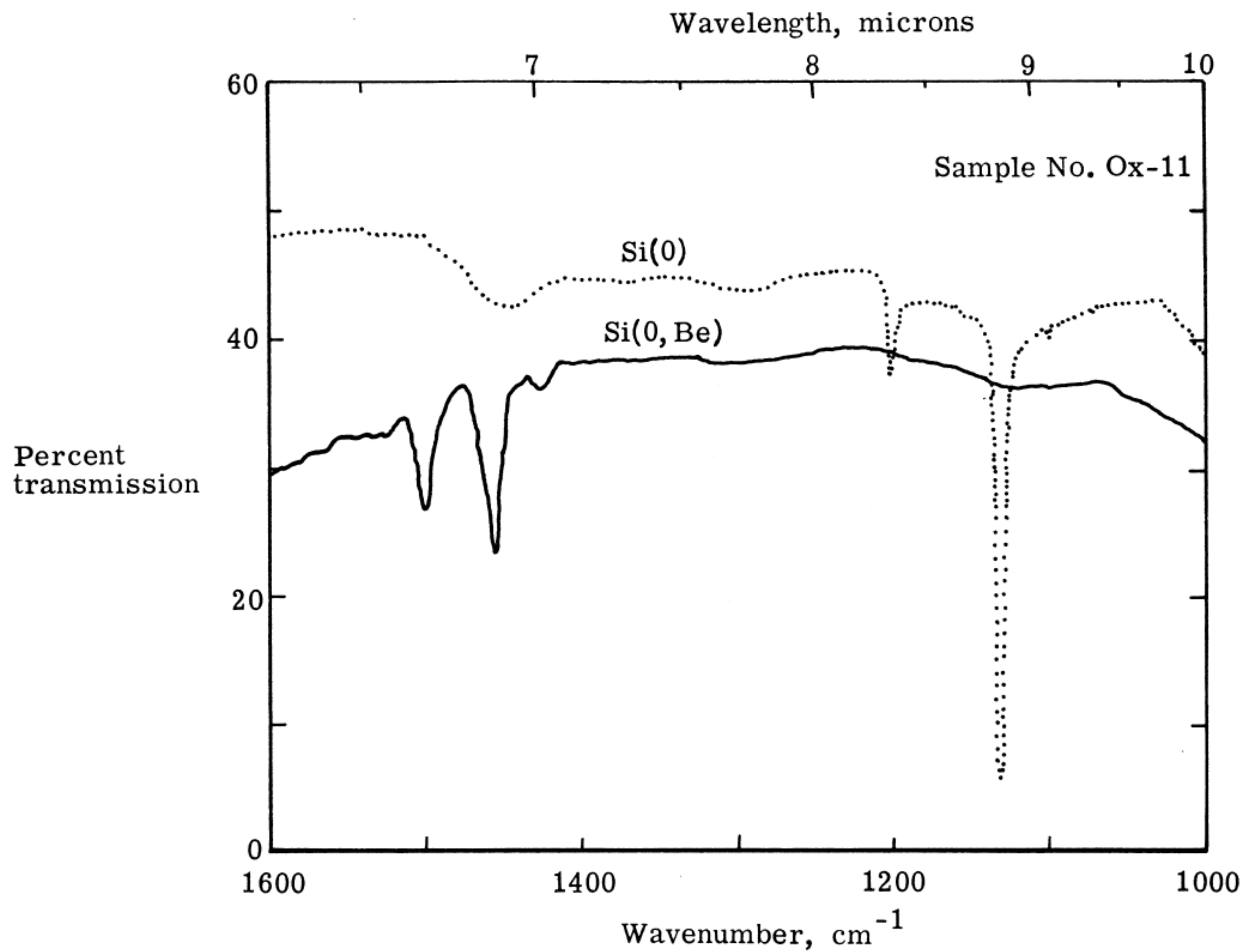

Figure 10.- Effect of beryllium on oxygen in Czochralski-grown silicon.

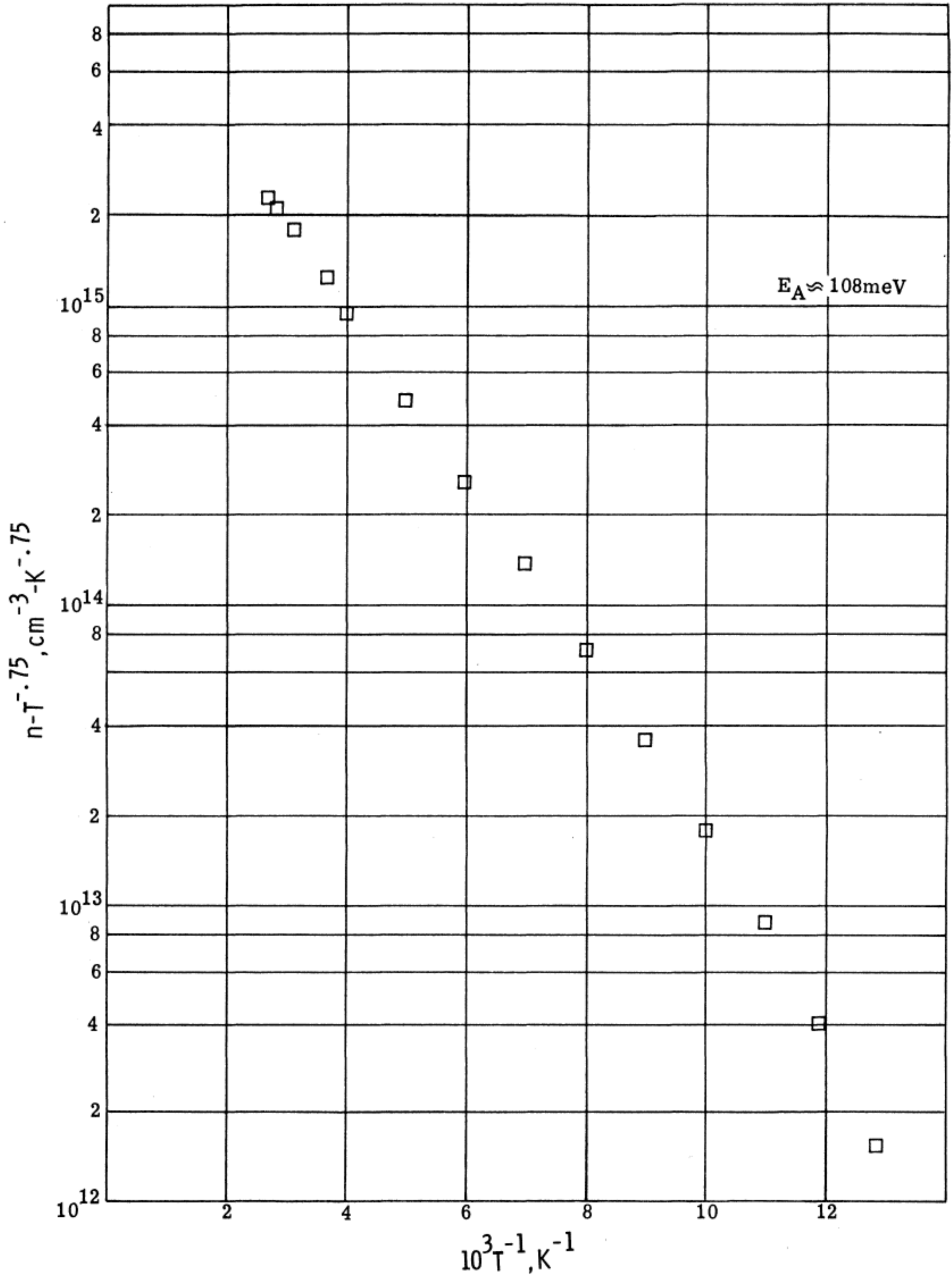

Figure 11.- Parameter containing carrier concentration and temperature as a function of temperature for a beryllium-lithium sample.

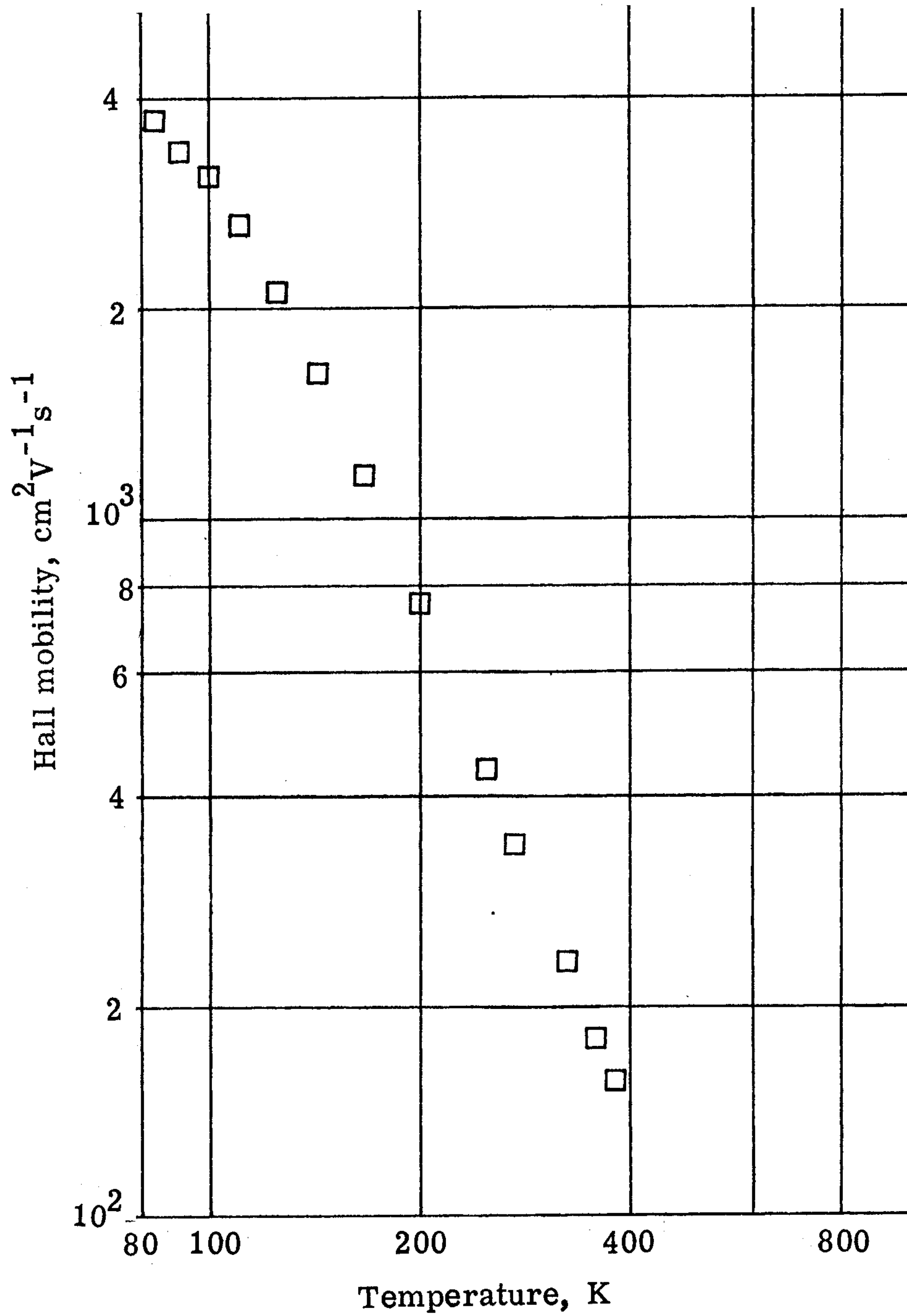

Figure 12.- Hall mobility as a function of temperature for a beryllium-lithium sample.

The suspicions that the introduction of lithium had caused something unusual were verified when the infrared spectrum of a beryllium-lithium doped sample was observed. As shown in figure 13, two new series of acceptor-like absorptions were observed at ionization energies corresponding to 106 and 81 meV, respectively. The previously observed Be spectra were still there. In addition, the absorption around 500 cm^{-1} was asymmetric and had its minimum value at about 516 cm^{-1}.

The spacings between the lines of all four excited state series are almost identical (cf. table 2). After quenching a Be + Li series from 600° C or greater, the intensities of the Set II lines are greatly reduced while the intensities of the Set I Be + Li series increase a little (see fig. 14). Similarly with a slow cool from 600° C, the Set II Be + Li absorptions are increased while the Set I decreases very little.

As with the beryllium samples, the absorptions associated with Be + Li broaden rapidly with increasing temperature and are unresolvable at temperatures greater than about 60° K to 70° K. However, as the sample temperature is increased, another series of lines appear which are displaced from the Set I Be + Li series by about 1.2 meV (see fig. 15).

The absorptions associated with Set II Be + Li do not seem to broaden as rapidly and do not show the second series. The appearance of the small absorptions in the Set I Be + Li is consistent with what would be expected if the fourfold degenerate ground state were split

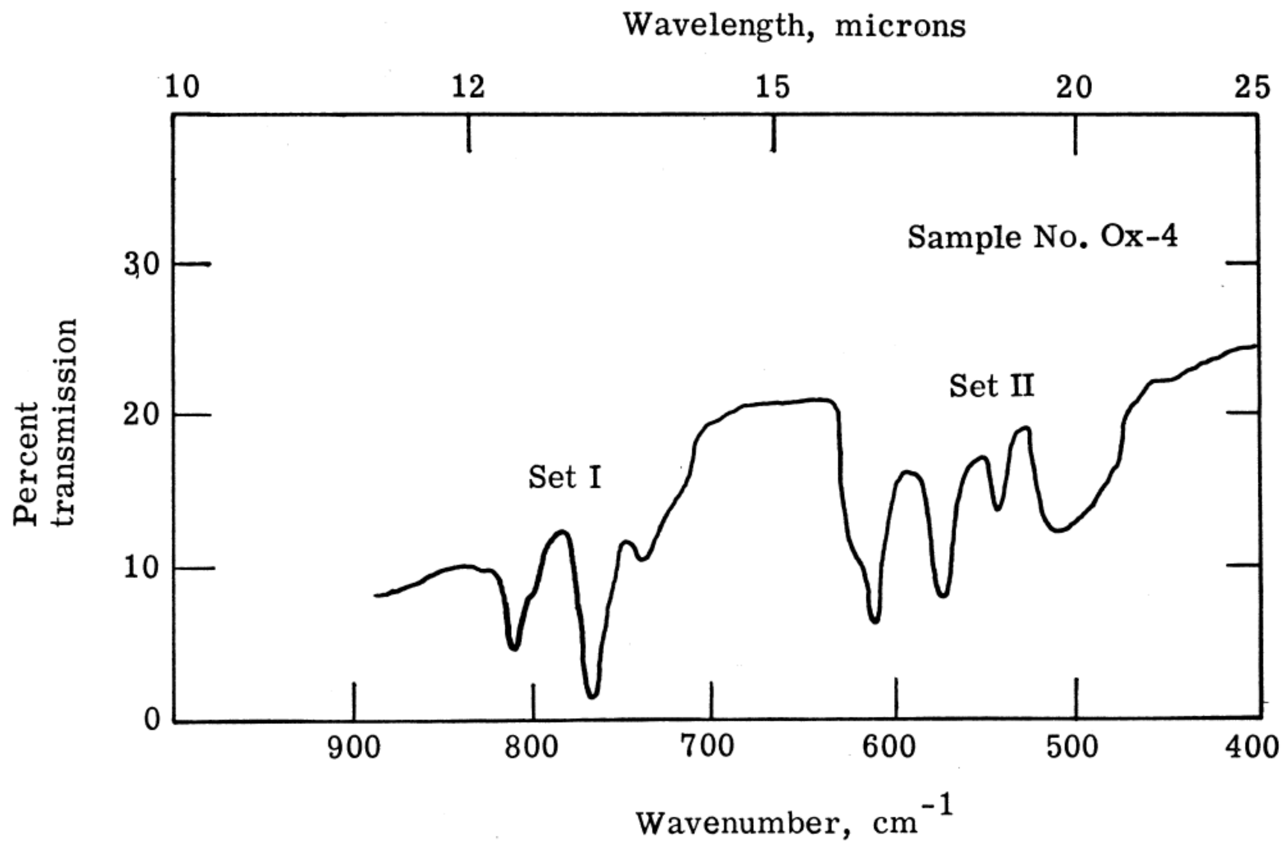

Figure 13.- Typical spectrum showing Set I and Set II beryllium-lithium absorptions.

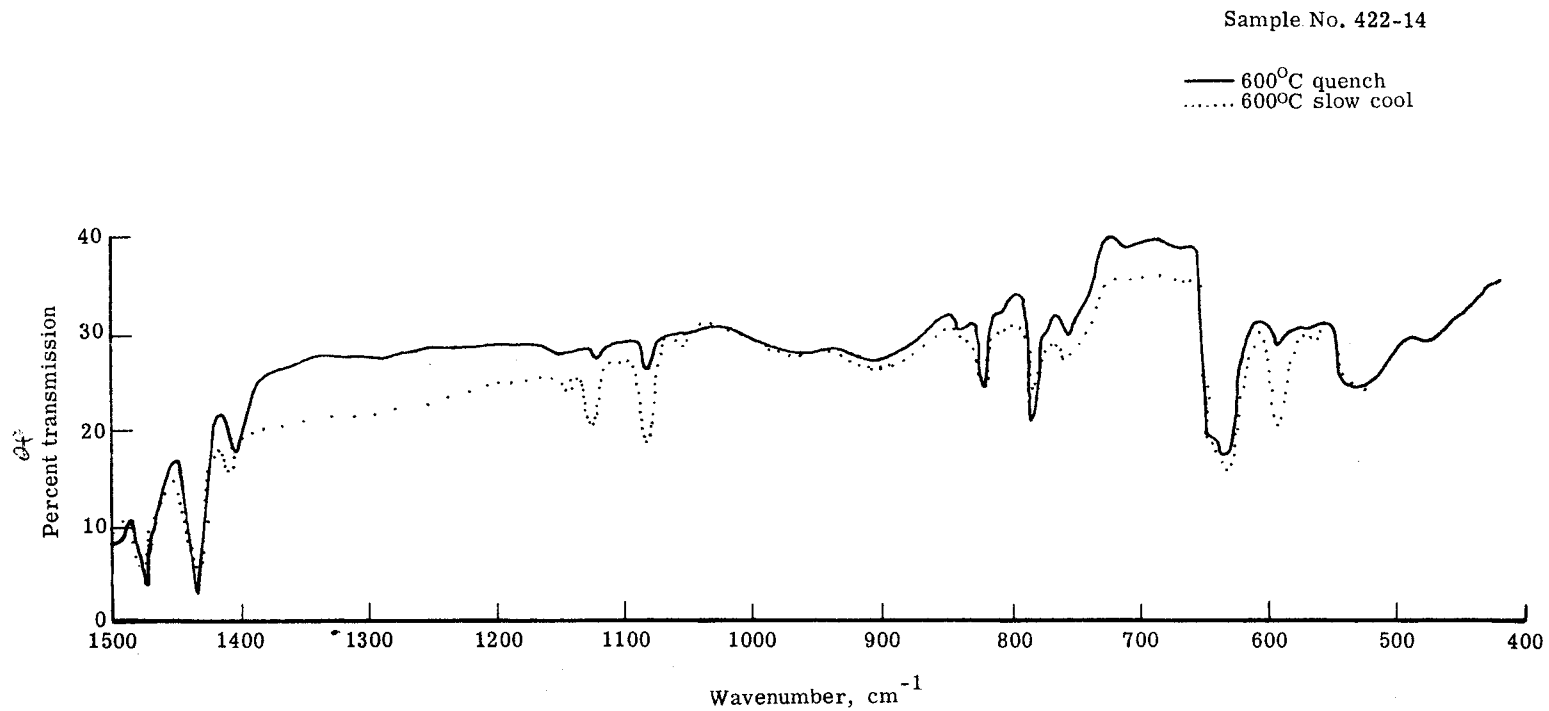

Figure 14.- Effects of quenching and annealing on Set I and Set II beryllium-lithium absorptions.

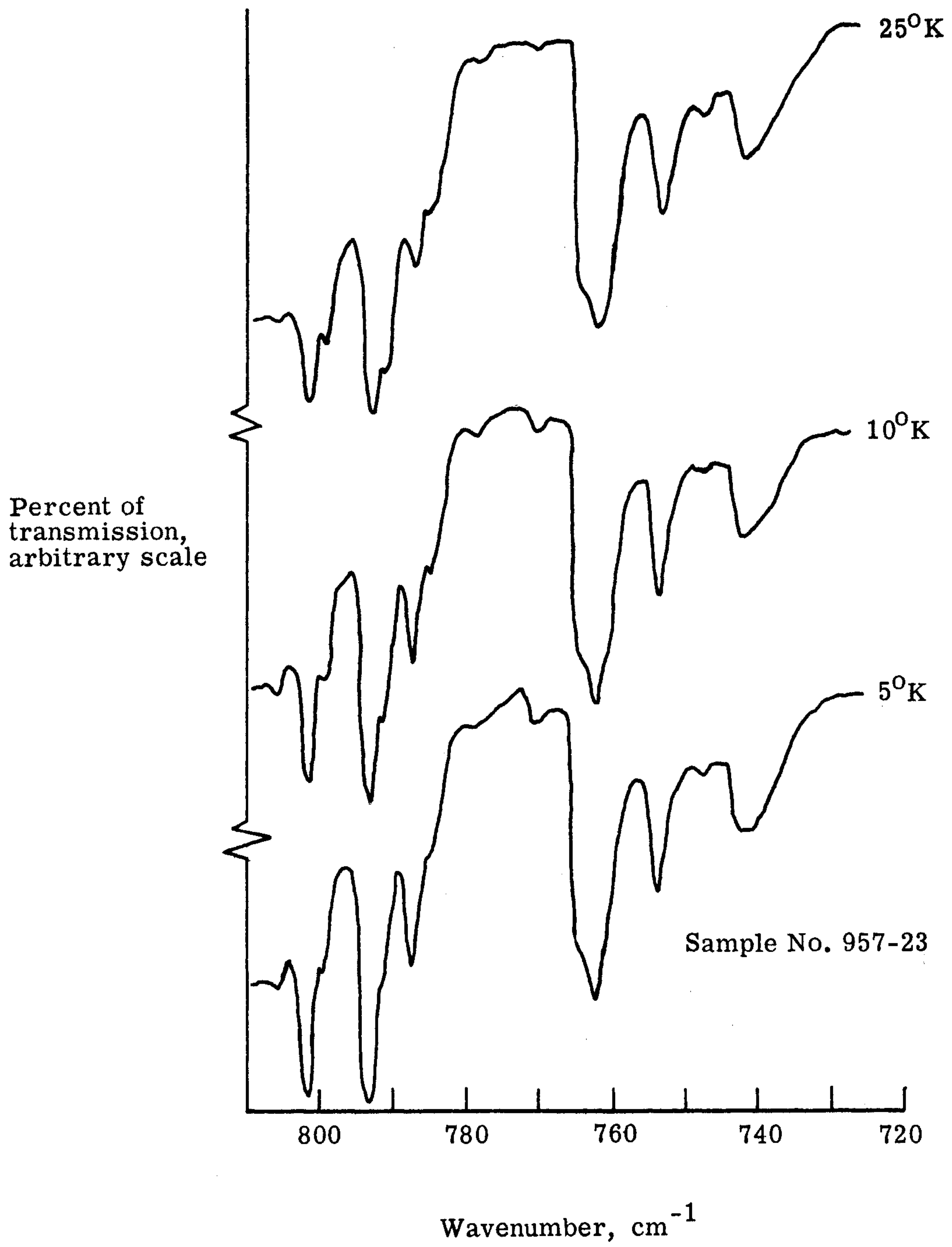

Figure 15.- Temperature dependence of Set I and Set II beryllium-lithium absorptions.

into two levels separated by 1.2 meV. As the temperature is raised, the upper level is populated by thermal excitation of the holes, and the transitions to the excited states can then be observed.

When lithium is introduced into a beryllium doped Czochralski silicon sample, the Be + Li spectra are essentially the same as for the float-zone material. The spectra for a Czochralski sample is shown in figure 13. The Set II Be + Li lines are broad and in the vicinity of strong lattice absorptions which make accurate determination of the spacings very difficult. It is felt that comparative spectra may be the best way to study this series of absorptions accurately.

V. PROPOSED MODELS

BERYLLIUM

Set I.- When beryllium is introduced into silicon, it produces a p-type material. The very fast diffusion rate of beryllium in silicon would lead one to expect that it would be an interstitial impurity; however, the beryllium that is electrically and optically observable apparently goes into a substitutional position. Mass spectroscopy data indicates that only about 10 percent of the beryllium in silicon contributes to the change in the electrical and optical properties. [40] Doping temperatures are around 1300° C, where the concentration of vacancies is high; and it is believed then that the beryllium diffuses interstitially but some beryllium is trapped in these vacancies.

In a substitutional site, beryllium would satisfy two of the covalent bonds with nearest neighbor silicon atoms. This would leave two unsatisfied covalent bonds in the vicinity of the beryllium. One can compare this neutral state in a simplistic way to a helium atom where we consider two holes to be bound to the beryllium impurity (see fig. 16). The holes would usually be several atomic diameters away from the beryllium and should be described satisfactorily by effective mass theory using the coulombic potential reduced by the dielectric constant. Therefore, when one of the holes is raised to an excited state, the spectra should look essentially like a Group III shallow acceptor. This is presumably what gives rise to the Set I absorptions. In the present context, the beryllium atom appears to be

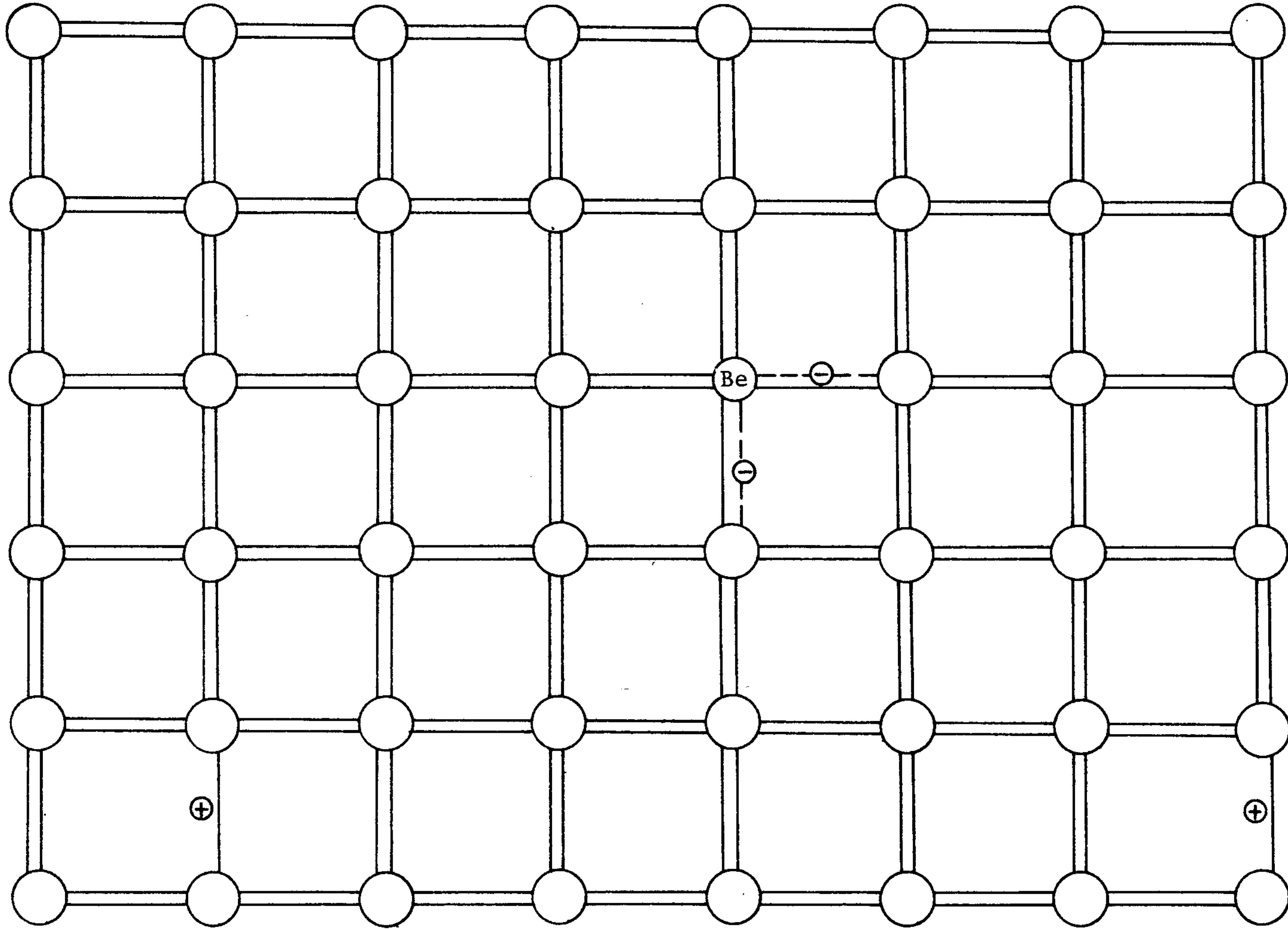

Figure 16.- Schematic model for neutral Set I beryllium.

significantly smaller than the silicon atom. According to the theory of Morgan,[15] this smaller atom will have a large local strain field associated with it which produces ground states much deeper than predicted by effective mass theory.

When one of the holes is freed, leaving an ionized center, simple theory would predict that the second hole should be observable at an energy somewhere around four times that required to free the first hole. This type of behavior has been observed for the donors magnesium and sulfur in silicon and the acceptor zinc in germanium. In the case of beryllium, however, no such second level has been observed in this region. Several things could explain the absence of the second series of absorptions associated with the Set I. One might start over by assuming that the beryllium is not in a substitutional site. This would require entirely new model concepts for the beryllium acceptor and would presumably complicate the model for the Be - Li complex. On this basis, another explanation is sought.

When the first hole is freed from the helium-like model, the second hole will be pulled into a smaller orbit (see fig. 17). It is clearly possible that when the orbit becomes smaller, the assumption of a constant dielectric constant used in effective mass theory becomes much weaker. The screening now seen by the hole could be much less than before, resulting in a much more tightly bound hole than predicted.

In addition, a lattice-symmetry short-range potential, "central cell potential," would be much more effective for a hole located close to the impurity site. This potential would be used for calculating

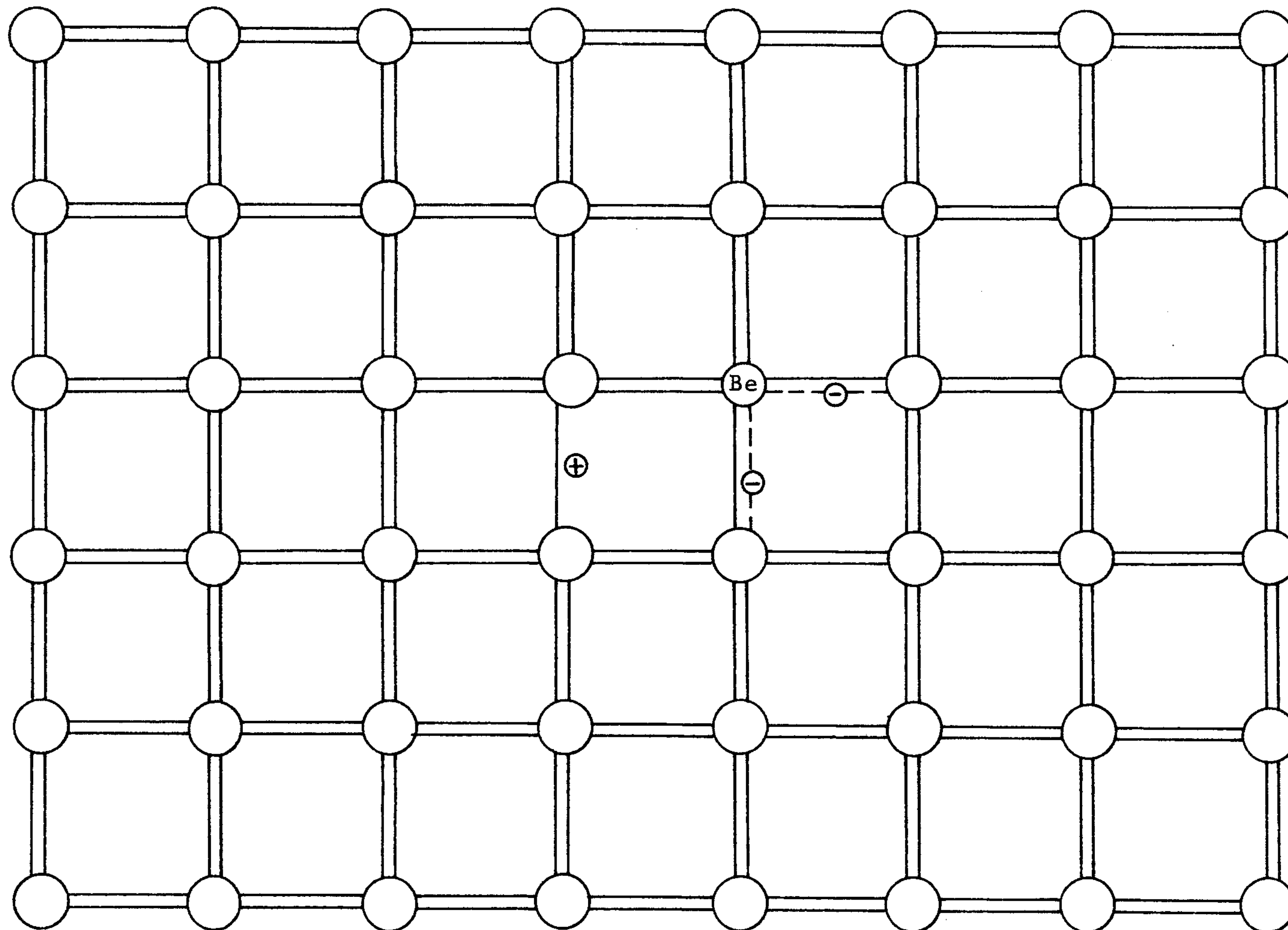

Figure 17.- Schematic model for singly ionized Set I beryllium.

the ground state energy for various impurities, and large values of the potential might possibly result in more tightly bound holes. In a theoretical paper, Ryabokon and Svidzinskii,[14] state that for Group II impurities, "... the effective short-range potential turns out to be more effective in them and leads to quite large level shifts. ... Furthermore, some of the deep impurity levels in silicon fall inside allowed energy bands." Thus, it seems possible for beryllium to be in a substitutional site, even though the second hole is not observed as predicted by the helium model.

Set II.- When a beryllium sample is quenched from high temperatures, the Set II absorptions are greatly reduced or disappear, and the Set I absorptions are enhanced. After a slow cool, the Set II absorptions are much stronger, and the Set I are slightly reduced. This seems to indicate that the Set II absorptions result from a more complex arrangement than Set I, and that Set I absorptions are due to a component of impurities giving rise to Set II. It seems to the author that the simplest model for the Set II absorptions are two beryllium atoms on nearest neighbor lattice sites. This configuration is somewhat similar to the divacancy bonding configurations, but less complex (see fig. 18). As the temperature of the sample is raised, the thermal energy of the impurity is such that the Set II sites are broken up into two Set I sites, that is, two substitutional beryllium sites. This results in low Set II absorptions after a quench. When the sample is slowly cooled, the beryllium atoms presumably tend to aggregate to relieve

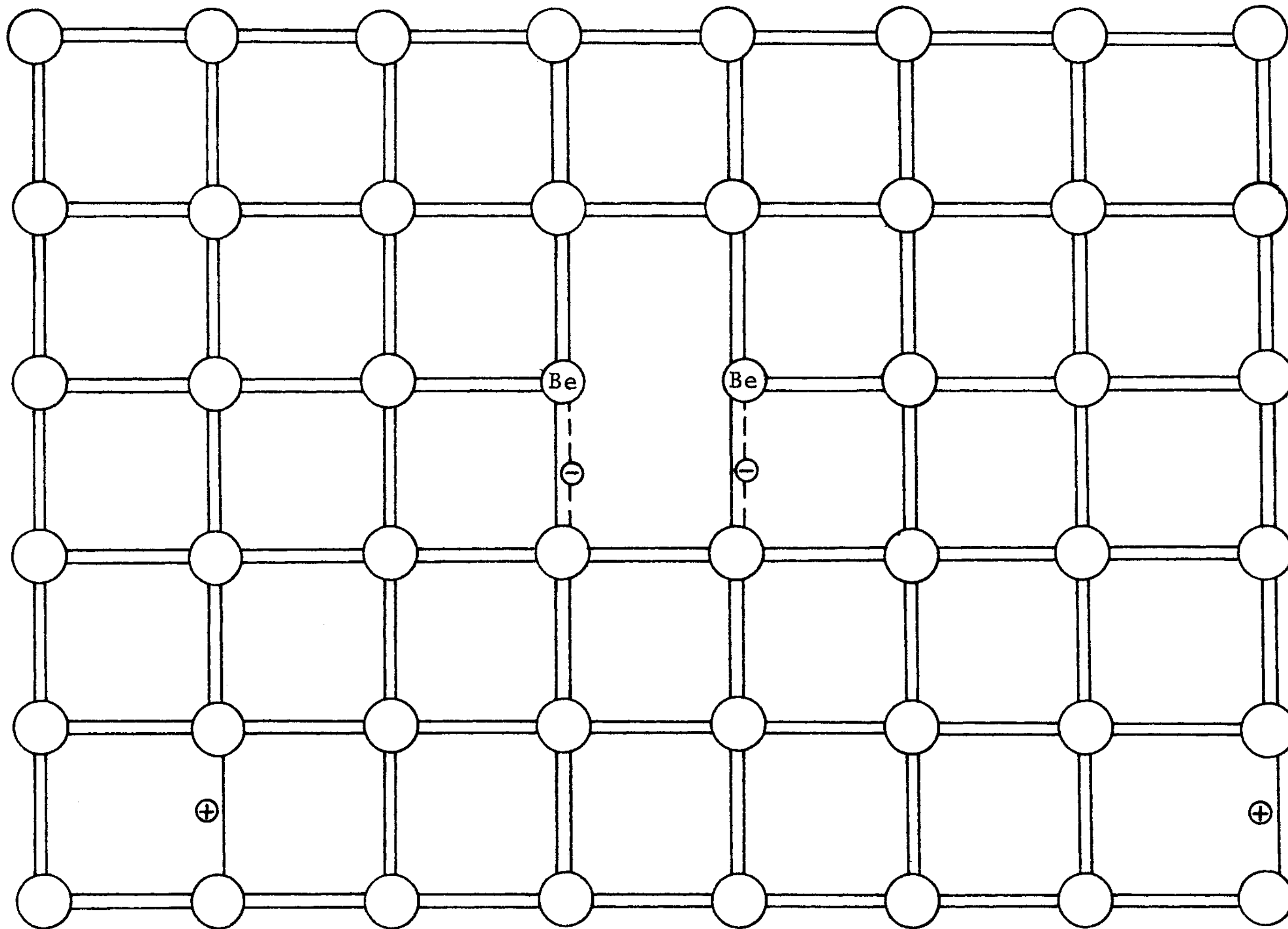

Figure 18.- Schematic model for neutral Set II beryllium.

crystal stresses around the small beryllium impurity; thus, more pairs are formed, and Set II absorptions are stronger after a slow cool. Again, the second hole associated with this model might not be observable in the infrared range (see fig. 19).

These two models seem to be consistent with the optical and electrical data.

BERYLLIUM AND LITHIUM

Set I.- When lithium is introduced into beryllium doped silicon, an acceptor level with almost identical spacings to the Set I beryllium spectrum has been observed, but with the binding energy of the hole reduced by about 80 percent. It is believed that the lithium goes into one of the nearest neighbor interstitial tetrahedral sites [21] and its valence electron satisfies one of the unsatisfied covalent silicon bonds (fig. 20). The lithium in this position could reduce the local strain field thus resulting in a lower ionization energy. [15] While the short-range effects of the lithium are apparently large, the long-range effects should be quite small; therefore, the excited states spectra should be essentially unaffected. Similarly, if the lithium is located in the immediate vicinity of the beryllium impurity, the ionic scattering from the complex center would be less than if the spacing between the two centers were large. That is, the beryllium + lithium center would be essentially a monovalent acceptor site.

As pointed out earlier, there is an apparent splitting of the ground state for the loosely bound hole in Be + Li samples. If the

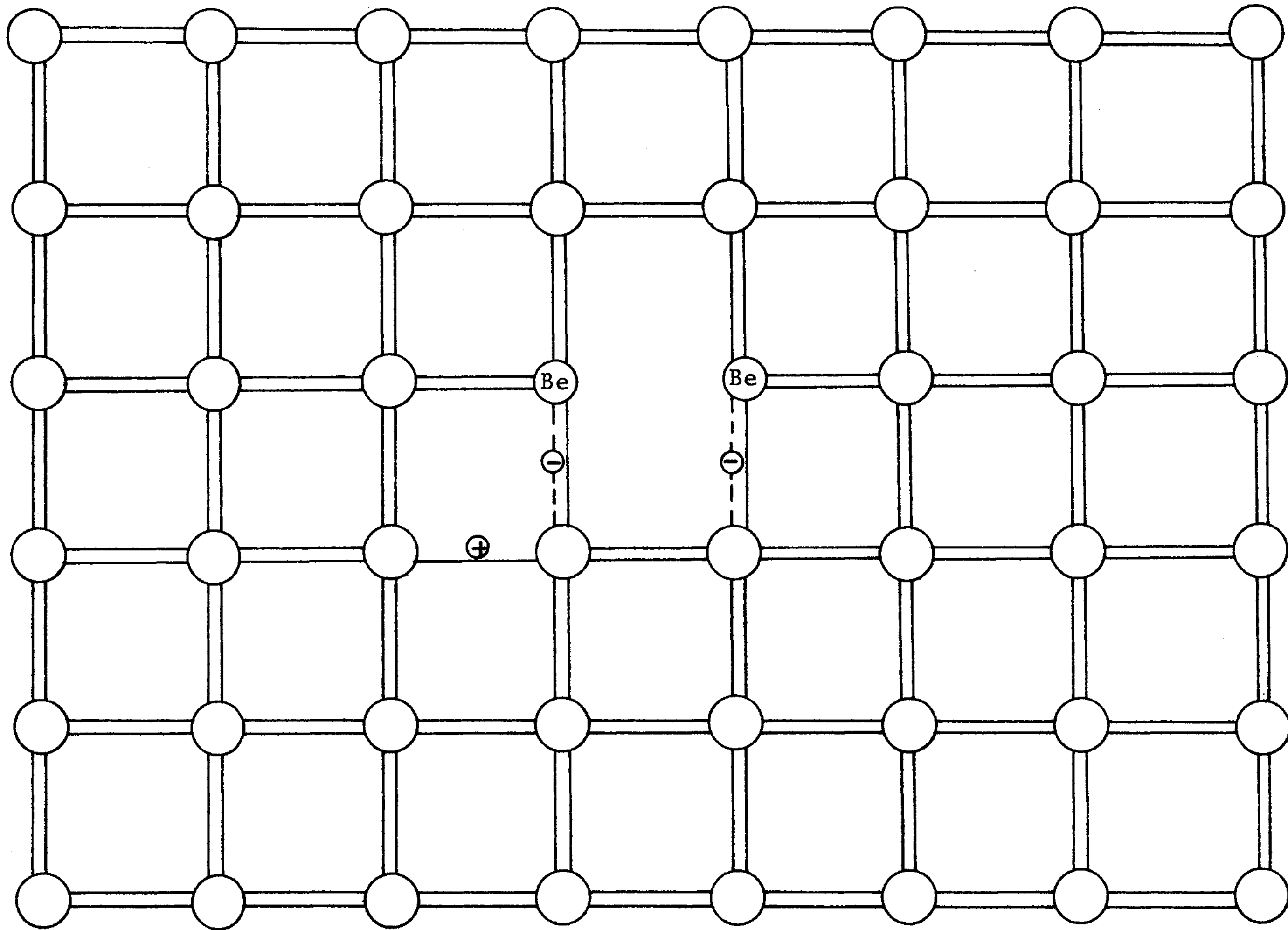

Figure 19.- Schematic model for singly ionized Set II beryllium.

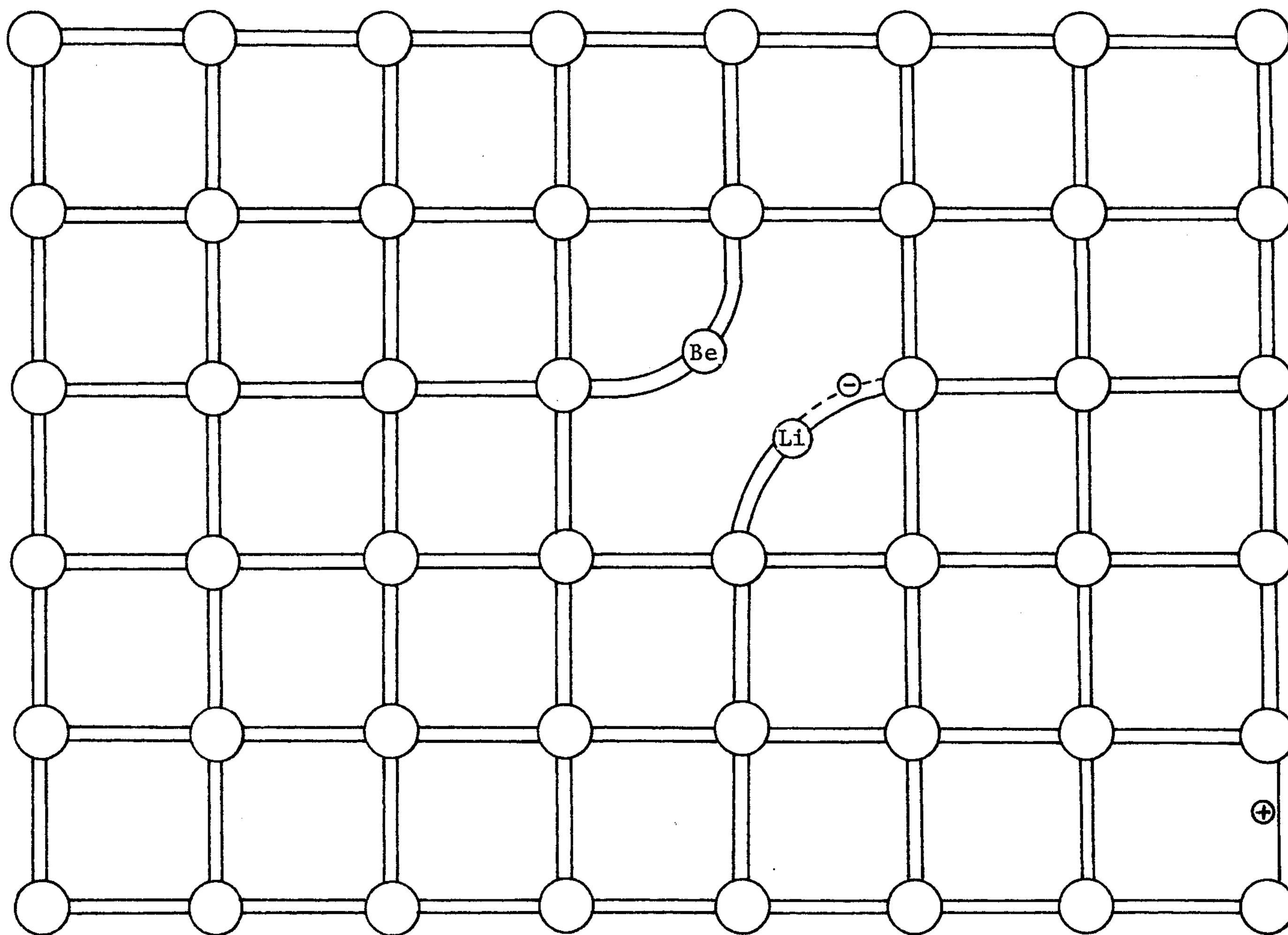

Figure 20.- Schematic model for netural beryllium-lithium complex, Set I.

lithium is in the immediate vicinity of the beryllium, the interaction between the beryllium and lithium ions would most likely be directed along a bond or < 111 > axis.[41] In effect, this would be equivalent to a uniaxial stress applied in the < 111 > direction. As reported by Onton, et al.,[8] a < 111 > stress causes the ground state to split into two levels. Since these stresses are local, the excited states would not be split. This is in agreement with what is observed.

Set II.- When lithium comes into the vicinity of the Set II beryllium, its valence electron again goes into one of the unsatisfied silicon convalent bonds, removing what would correspond to the deep hole (see fig. 21). The result, as before, would be to reduce the binding energy of the remaining hole. The mobility would not be affected by this configuration because no new ionic scattering centers have been introduced.

If this model is accurate, the complex would probably not have a < 111 > symmetry when the lithium is introduced; but the model for the Set II beryllium complex would have a < 111 > axis of symmetry. However, the ground state for a "helium-like" model would not have the same degeneracy as the Group III acceptors; and in fact, it is likely that both the Set I and Set II beryllium will have only twofold degenerate ground states.[41] The lithium should reduce even further the symmetry of the Set II beryllium center, but the ground state would probably remain twofold degenerate.[8]

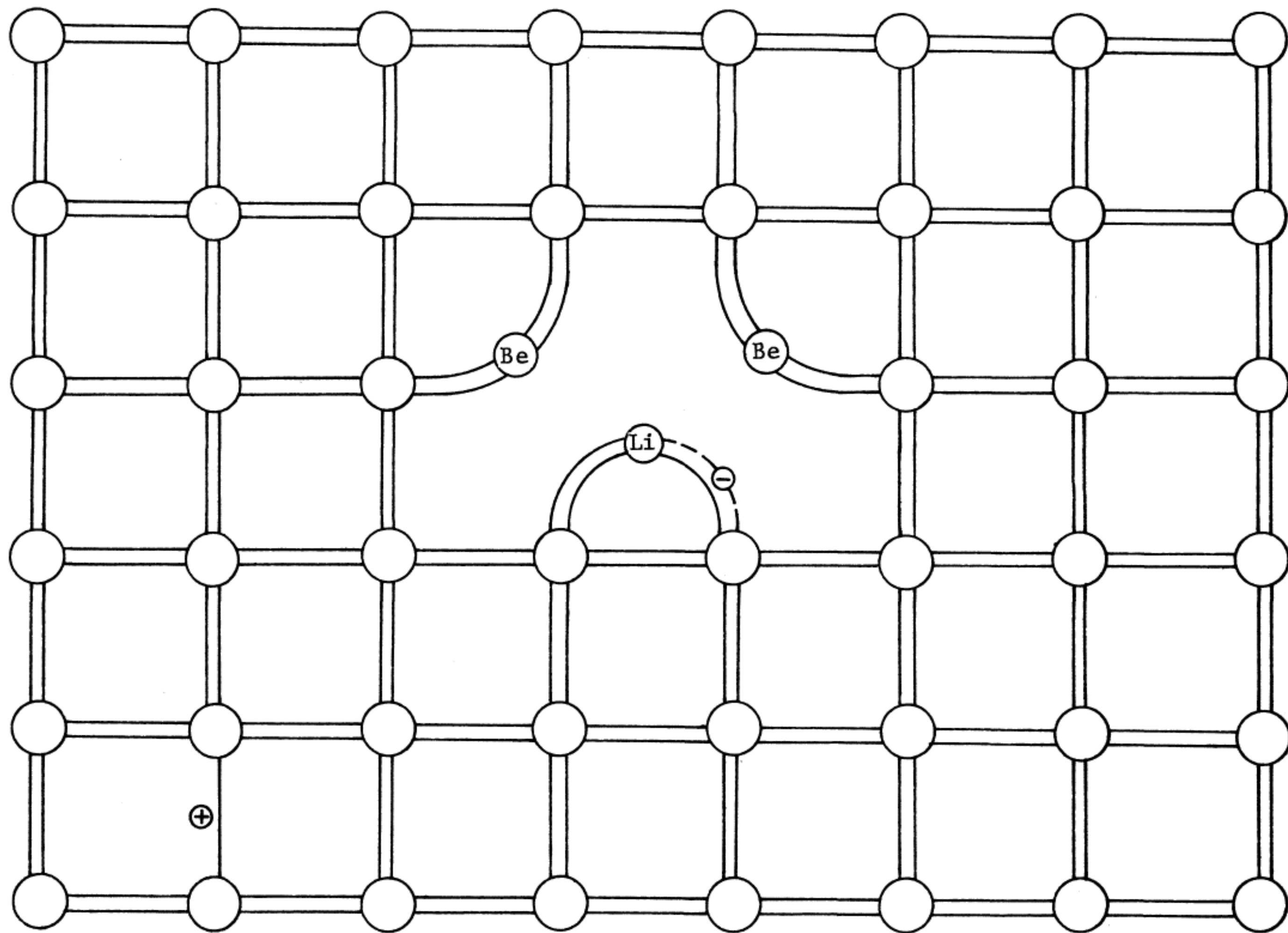

Figure 21.- Schematic model for neutral beryllium-lithium complex, Set II.

VI. SUMMARY

Beryllium as an impurity in silicon gives rise to two acceptor levels and associated excited states levels referred to as Set I and Set II. The ratio of the absorption coefficients between Set I and Set II can be changed by quenching or annealing. Analysis of these studies indicates that the Set II absorptions are due to an impurity complex, and that the Set I absorptions are due to a component of the Set II complex.

When lithium is introduced into the beryllium-silicon system it gives rise to two new acceptor levels. These levels behave under quenching and annealing just like the Set I and Set II beryllium levels. The Set I Be + Li ground state is split into two levels.

The following models, which seem to be the simplest impurity configurations that agree qualitatively with all the observations, are proposed for these four defects:

(a) Beryllium - Set I. This defect is a single substitutional beryllium impurity. The second hole of a helium-like model is so deeply bound that it cannot be found in the region predicted by shallow acceptor theory.

(b) Beryllium - Set II. This defect is made up of two beryllium atoms on nearest-neighbor substitutional sites. Again, a deep hole may be associated with the level; but the hole could be so deeply bound that it falls inside the allowed energy bands.

(c) Be + Li - Set I. The lithium ion is trapped in the immediate vicinity of the Set I beryllium and removes the deep hole. The

symmetry of the impurity site is reduced, resulting in the reduction of the degeneracy of the ground state and the splitting of this level.

(d) Be + Li - Set II. The lithium removes the deep hole as in Set I, but the ground state degeneracy is not reduced due to the different symmetries associated with the Set I and Set II, beryllium sites.

VII. REFERENCES

1. Pearson, G. L.; and Bardeen, J.: Electrical Properties of Pure Silicon and Silicon Alloys Containing Boron and Phosphorus. Phys. Rev., vol. 75, 1949, pp. 865-883.

2. Morin, F. J.; and Maita, J. P.: Electrical Properties of Silicon Containing Arsenic and Boron. Phys. Rev., vol. 96, 1954, pp. 28-35.

3. Morin, F. J.; Maita, J. P.; Shulman, R. G.; and Hannay, N. B.: Impurity Levels in Silicon. Phys. Rev., vol. 96, 1954, p. A933.

4. Long, Donald; and Myers, John: Hall Effect and Impurity Levels in Phosphorus-Doped Silicon. Phys. Rev., vol. 115, 1959, pp. 1119-1121.

5. Hrostowski, H. J.; and Kaiser, R. H.: Infrared Spectra of Group III Acceptors in Silicon. J. Phys. Chem. Solids, vol. 4, 1958, pp. 148-153.

6. Picus, G.; Burstein, E.; and Henvis, B.: Absorption Spectra of Impurities in Silicon - II Group V Donors. J. Phys. Chem. Solids, vol. 1, 1956, pp. 75-81.

7. Aggarwal, R. L.; and Ramdas, A. K.: Effect of Uniaxial Stress of the Excitation Spectra of Donors in Silicon. Phys. Rev., vol. 137, 1965, pp. A602-612.

8. Onton, A.; Fisher, P.; and Ramdas, A. K.: Spectroscopic Investigation of Group III Acceptor States in Silicon. Phys. Rev., vol. 163, 1967, pp. 686-703.

9. Kohn, W.; and Luttinger, J. M.: Theory of Donor States in Silicon. Phys. Rev., vol. 98, 1955, pp. 915-922.

10. Kleiner, W. H.: Excited Donor Levels in Silicon. Phys. Rev., vol. 97, 1955, pp. 1722-1723.

11. Schechter, D.: Theory of Shallow Acceptor States in Silicon and Germanium., J. Phys. Chem. Solids, vol. 23, 1962, pp. 237-247.

12. Kohn, W.: Shallow Impurity States in Silicon and Germanium. Solid State Physics, vol. 5, 1957, pp. 257-320.

13. Narita, Koziro; and Shimizu, Tatsuo: Ground State Energies of Donors in Germanium and Silicon. J. Phys. Soc. Japan, vol. 16, 1961, p. 2588.

14. Ryabokon, V. N.; and Svidzinskii, K. K.: Theory of Deep Acceptor Levels in Semiconductors. Soviet Phys. - Solid State, vol. 11, 1969, pp. 473-478.

15. Morgan, T. N.: Shallow Acceptor States in Semiconductors - The Local Strain Field. 10th Int. Conf. on Physics of Semiconductors, Cambridge, Mass. paper TPa-4, Aug. 1970.

16. Kaiser, W.; and Keck, P. H. Oxygen Content of Silicon Single Crystals. Journal of Applied Physics, vol. 28, 1957, pp. 882-887.

17. Hrostowski, H. J.; and Kaiser, R. H.: Infrared Absorption of Oxygen in Silicon. Phys. Rev., vol. 107, 1957, pp. 966-972.

18. Hrostowski, H. J.; and Adler, B. J.: Evidence for Internal Rotation in the Fine Structure of the Infrared Absorption of Oxygen in Silicon. The Journal of Chemical Physics, vol. 33, 1960, pp. 980-990.

19. Crouch, R. K.; Gilmer, T. E., Jr.; and Franks, R. K.: Thermal Ionization Energy of Lithium and Lithium-Oxygen Complexes in Single-Crystal Silicon. J. Phys. Chem. Solids, vol. 30, 1969, pp. 2037-2043.

20. Gilmer, T. E., Jr.; Franks, R. K.; and Bell, R. J.: An Optical Study of Lithium and Lithium-Oxygen Complexes as Donor Impurities in Silicon. J. Phys. Chem. Solids, vol. 26, 1965, pp. 1195-1204.

21. Aggarwal, R. L.; Fisher, P.; Mourzine, V.; and Ramdas, A. K.: Excitation Spectra of Lithium Donors in Si and Ge. Phys. Rev., vol. 138, 1965, pp. A882-893.

22. Pell, E. M.: Interactions Between Li and O in Si. Solid State Physics in Electronics and Telecommunications, vol. 1, Academic Press, New York, 1960, pp. 261-276.

23. Chrenko, R. M.; McDonald, R. S.; and Pell, E. M.: Vibrational Spectra of Lithium-Oxygen and Lithium-Boron Complexes in Silicon. Phys. Rev., vol. 138, 1965, pp. A1775-1784.

24. Balkanski, M.; and Nazarewicz, W.: Localized Vibration Due to Boron and Lithium in the Silicon Lattice. J. Phys. Chem. Solids, vol. 25, 1964, pp. 437-441.

25. Waldner, M.; Hiller, M. A.; and Spitzer, W. G.: Infrared Combination Mode Absorption in Lithium-Boron-Doped Silicon. Phys. Rev., vol. 140, 1965, pp. A172-176.

26. Newman, R. C.; and Smith, R. S.: Vibrational Absorption of Carbon and Carbon-Oxygen Complexes in Silicon. J. Phys. Chem. Solids, vol. 30, 1969, pp. 1493-1505.

27. Tyapkina, N. D.; Krivopolenova, M. M.; and Vavilov, V. S.: Electrical Properties of p-type Germanium Containing Beryllium. Soviet Physics-Solid State, vol. 6, 1965, pp. 1732-1733.

28. Sidorov, V. I.; Sushko, T. E.; and Shulman, A. Ya.: Investigation of Optical Absorption in Germanium Doped with Zinc and Compensated with Antimony. Soviet Physics - Solid State, vol. 8, 1967, pp. 1608-1610.

29. Fisher, P.; and Fan, H. Y.: Absorption Spectra and Zeeman Effect of Copper and Zinc Impurities in Germanium. Phys. Rev. Letters, vol. 5, 1960, pp. 195-197.

30. Robertson, J. B.; and Franks, R. K.: Beryllium as an Acceptor in Silicon. Solid State Communications, vol. 6, 1968, pp. 825-826.

31. Robertson, J. B.: The Effect of Beryllium on Oxygen in Silicon. Bull. Am. Phys. Soc., vol. 13, 1968, p. A1475.

32. Franks, R. K.; and Robertson, J. B.: Magnesium as a Donor Impurity in Silicon. Solid State Commun., vol. 5, 1967, pp. 479-481.

33. Ho, L. T.; and Ramdas, A. K.: Excitation Spectra and Piezospectroscopic Effects of Neutral and Singly-Ionized Magnesium Donors in Silicon. To be published.

34. Taft, E. A.; and Carlson, R. O.: Beryllium as an Acceptor in Silicon. J. Electrochem. Soc. Solid State Science, vol. 117, 1970, pp. 711-713.

35. Krag, W. E.; Kleiner, W. H.; Zeiger, H. J.; and Fischler, S.: Sulfur Donors in Silicon: Infrared Transitions and Effects of Calibrated Uniaxial Stress. J. Phys. Soc. Japan, vol. 21, 1966, pp. 230-233.

36. Valdes, L. B.: Resistivity Measurements on Germanium for Transistors. Proc. of the I.R.E., vol. 42, 1954, pp. 420-427.

37. Schultz, M. L.: Silicon: Semiconductor Properties. Infrared Physics, vol. 4, 1964, pp. 93-112.

38. Bauman, Robert P.: Absorption Spectroscopy. John Wiley and Sons, N. Y., 1962.

39. McKelvey, John P.: Solid State and Semiconductor Physics. Harper and Row, N. Y., 1966, pp. 308 ff.

40. Robertson, J. B.: Private communication.

41. Morgan, T. N.: Private communication.

XIII. ACKNOWLEDGEMENTS

The author wishes to express his thanks to Dr. T. E. Gilmer, Jr. for his assistance as an adviser and consultant during the course of this work. The suggestion of this topic by Dr. J. B. Robertson is greatly appreciated. He has sacrificed a great deal of his work and time in order that the author might do this thesis. Mr. M. F. McNear was very helpful in assisting with sample preparation and equipment construction or modification. The author also wishes to thank Dr. T. N. Morgan for a discussion of and comments on the results. This work was supported by NASA, Langley Research Center and the author is grateful to them for allowing him to do the work and use the results. Finally, the author wishes especially to express appreciation to his wife, Ann, for her unfailing encouragement and moral support.

The vita has been removed from the scanned document

A STUDY OF BERYLLIUM AND BERYLLIUM-LITHIUM COMPLEXES IN SINGLE-CRYSTAL SILICON

By Roger K. Crouch

ABSTRACT

When beryllium is thermally diffused into silicon, it gives rise to acceptor levels 191 meV and 145 meV above the valence band. Quenching and annealing studies indicate that the 145 meV level is due to a more complex beryllium configuration than the 191 meV level. When lithium is thermally diffused into a beryllium doped silicon sample it produces two new acceptor levels at 106 meV and 81 meV. Quenching and annealing studies indicate that these new levels are due to lithium forming a complex with the defects responsible for the 191 meV and 145 meV beryllium levels, respectively. Electrical measurements imply that the lithium impurity ions are physically close to the beryllium impurity atoms. The ground state of the 106 meV beryllium-lithium level is split into two levels, presumably by internal strains. Tentative models are proposed to explain these results.